

DDC FILE COPY

AD A0 66 598

LEVEL

CO15805

SC



RADC-TR-78-285
Interim Report
January 1979

ANALYSIS OF TECHNIQUES FOR IMAGING THROUGH THE ATMOSPHERE

The Optical Sciences Company

Sponsored by
Defense Advanced Research Projects Agency (DoD)
ARPA Order No. 2646

DDC
RECEIVED
MAR 30 1979
SC

APPROVED FOR PUBLIC RELEASE; DISTRIBUTION UNLIMITED

The views and conclusions contained in this document are those of the authors and should not be interpreted as necessarily representing the official policies, either expressed or implied, of the Defense Advanced Research Projects Agency or the U. S. Government.

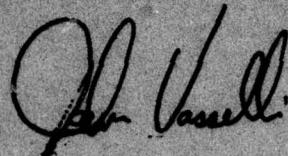
ROME AIR DEVELOPMENT CENTER
Air Force Systems Command
Griffiss Air Force Base, New York 13441

79 03 29 027

This report has been reviewed by the RADC Information Office (OI) and is releasable to the National Technical Information Service (NTIS). At NTIS it will be releasable to the general public, including foreign nations.

RADC-TR-78-285 has been reviewed and is approved for publication.

APPROVED:


JOHN J. VASSELLI
Project Engineer

If your address has changed or if you wish to be removed from the RADC mailing list, or if the addressee is no longer employed by your organization, please notify RADC (OCSE) Griffiss AFB NY 13441. This will assist us in maintaining a current mailing list.

MISSION
of
Rome Air Development Center

RADC plans and conducts research, exploratory and advanced development programs in command, control, and communications (C³) activities, and in the C³ areas of information sciences and intelligence. The principal technical mission areas are communications, electromagnetic guidance and control, surveillance of ground and aerospace objects, intelligence data collection and handling, information system technology, ionospheric propagation, solid state sciences, microwave physics and electronic reliability, maintainability and compatibility.



ANALYSIS OF TECHNIQUES FOR IMAGING
THROUGH THE ATMOSPHERE

Dr. David L. Fried

Contractor: the Optical Sciences Company
Contract Number: F30602-77-C-0021
Effective Date of Contract: 1 October 1976
Contract Expiration Date: 1 April 1979
Short Title of Work: Analysis of Techniques for Imaging
Through the Atmosphere
Program Code Number: 7E20
Period of Work Covered: Apr 78 - Oct 78

Principal Investigator: Dr. David L. Fried
Phone: 714 524-3622

Project Engineer: John Vasselli
Phone: 315 330-3148

Approved for public release; distribution unlimited.

This research was supported by the Defense Advanced
Research Projects Agency of the Department of
Defense and was monitored by John J. Vasselli (OCSE)
Griffiss AFB NY 13441 under Contract F30602-77-C-0021.

79 03 29 027

UNCLASSIFIED

SECURITY CLASSIFICATION OF THIS PAGE (When Data Entered)

REPORT DOCUMENTATION PAGE		READ INSTRUCTIONS BEFORE COMPLETING FORM
1. REPORT NUMBER RADC TR-78-285	2. GOVT ACCESSION NO.	3. RECIPIENT'S CATALOG NUMBER
4. TITLE (and Subtitle) ANALYSIS OF TECHNIQUES FOR IMAGING THROUGH THE ATMOSPHERE		5. TYPE OF REPORT & PERIOD COVERED Final Interim Report, no. 4, Apr - Oct 78
7. AUTHOR(s) Dr. David L. Fried	8. CONTRACT OR GRANT NUMBER(s) F30602-77-C-0021	9. PROGRAM ELEMENT, PROJECT, TASK AREA & WORK UNIT NUMBERS 2646
9. PERFORMING ORGANIZATION NAME AND ADDRESS The Optical Sciences Company P.O. Box 446 Placentia CA 92670	10. CONTROLLING OFFICE NAME AND ADDRESS Defense Advanced Research Projects Agency 1400 Wilson Blvd Arlington VA 22209	11. SECURITY CLASS. (of this report) UNCLASSIFIED
14. MONITORING AGENCY NAME & ADDRESS (if different from Controlling Office) Rome Air Development Center (OCSE) Griffiss AFB NY 13441.	15. DECLASSIFICATION/DOWNGRADING SCHEDULE N/A	
16. DISTRIBUTION STATEMENT (of this Report) Approved for public release; distribution unlimited.		
17. DISTRIBUTION STATEMENT (of the abstract entered in Block 20, if different from Report) Same		
18. SUPPLEMENTARY NOTES RADC Project Engineer: Mr. John Vasselli (OCSE)		
19. KEY WORDS (Continue on reverse side if necessary and identify by block number) Speckle interferometry Labeyrie technique speckle imagery Knox-Thompson algorithm atmospheric turbulence isoplanatism		
20. ABSTRACT (Continue on reverse side if necessary and identify by block number) A detailed analysis of turbulence effects in speckle interferometry, i.e., the Labeyrie technique, and in speckle imagery, the Knox-Thompson algorithm, is presented. Particular concern is devoted to the problem of isoplanatism, as originally we had thought that the Knox-Thompson algorithm might have a very large isoplanatic field-of-view. Our analytic results show that the isoplanatic patch size is approximately the same for Knox-Thompson and Labeyrie methods, and nearly the same as for adaptive optics. It is noted that, unlike the adaptive		

DD FORM 1 JAN 73 1473 EDITION OF 1 NOV 65 IS OBSOLETE

UNCLASSIFIED

SECURITY CLASSIFICATION OF THIS PAGE (When Data Entered)

391 358

Jm

→ next page

UNCLASSIFIED

SECURITY CLASSIFICATION OF THIS PAGE(When Data Entered)

optics systems for which the ability to record high spatial frequency details is lost due to anisoplanatism, for the speckle methods anisoplanatism does not suppress the high spatial frequency details of the image - it merely jumbles them so that no real information is developed. From these results, it appears that a direct application of speckle techniques will not provide a significant relief from the anisoplanatism problems of adaptive optics.

As part of the analysis of the Knox-Thompson method, we develop the conditions for the allowable spatial frequency separation (something done previously only by simulation). We find that the allowable spatial frequency separation should be less than $0.427 \frac{r_0}{\lambda}$, and preferably should be less than $0.2 \frac{r_0}{\lambda}$.

$r \text{ sub } \phi / \lambda \text{ m b d a}$

SECURITY CLASSIFICATION OF THIS PAGE(When Data Entered)

TABLE OF CONTENTS

<u>Section</u>	<u>Title</u>	<u>Page</u>
1	Introduction	1
2	Labeyrie Technique: Single Point Source	4
3	Labeyrie Technique: Two Point Sources	17
4	Labeyrie Technique: Anisoplanatism	26
5	Knox-Thompson Algorithm: Isoplanatism Assumed	35
6	Knox-Thompson Algorithm: Anisoplanatism	44
	References	55
	Appendix A, Monte Carlo Integral Evaluation	57
	Appendix B, Computer Program Listings	68

ACCESSION for

NTIS ☒ White Section

DOC ☐ Buff Section

UNANNOUNCED

JUSTIFICATION

BY DISTRIBUTION/AVAILABILITY CODES

Di ☐ SPECIAL

A

LIST OF FIGURES

<u>Figure No.</u>	<u>Title</u>	<u>Page</u>
1	Speckle Transfer Function for $D/r_0 = 10$.	49
2	Speckle Transfer Function for $D/r_0 = 30$.	50
3	Speckle Transfer Function for $D/r_0 = 100$.	51
4	Speckle Transfer Function for $D/r_0 = 300$.	52
5	Speckle Transfer Function for $D/r_0 = 1000$.	53
6	Vertical Distribution of the Refractive- Index Structure Constant.	54

LIST OF TABLES

<u>Table No.</u>	<u>Title</u>	<u>Page</u>
A.1	Speckle Transfer Function, Monte Carlo Results	66
A.2	Monte Carlo Error Parameters	67

1. Introduction

Isoplanatism, as it is conventionally used, refers to the uniformity of the quality of imagery over some portion of a focal plane. Introduced into the literature in this form, it serves to "validate" the concept of the modulation transfer function. Its meaning is physically straightforward and intuitively quite clear. But the concept of isoplanatism as applied to special imaging-through-turbulence concepts is a much more complex matter. Here, rather than defining the focal plane uniformity of image quality, it is directly tied to the achievability of image quality.

Our reference to special imaging-through-turbulence concepts is meant to include adaptive optics and the two speckle imagery techniques, the first demonstrated by Labeyrie¹ and the second conceived and analyzed by Knox and Thompson.² (Analysis of the amplitude interferometer concept of Currie³ can probably be obtained as a special case of the speckle interferometer, but we shall not explicitly concern ourselves with this here.) Adaptive optics and speckle imagery have the highly significant feature that they sense the received wavefront in time periods shorter than that in which the atmospheric turbulence-induced wavefront distortion can change. Isoplanatism for these special imaging techniques refers to the dependence on field-angle of the wavefront distortion (rather than to the dependence on field-angle of the image quality). With these special imaging techniques, if the wavefront distortion is nearly the same for a large enough range of field-angles, the "ideal" resolution can be achieved, no matter how severe the actual wavefront distortion per se is.

We have elsewhere^{4,5} presented an analysis of the isoplanatic considerations in adaptive optics, and therefore will not treat that problem here. In this work, we shall restrict our attention to isoplanatic effects in speckle interferometry (the Labeyrie technique) and in speckle imagery (the Knox-Thompson concept). In the next two sections, we shall examine

the Labeyrie technique in the absence of isoplanatism effects. This will establish the basis for our subsequent analysis. The first of these two sections, i.e., Section 2, will treat a single point source (a situation in which there is manifestly no anisoplanatism effect), and will closely parallel the analysis of Korif.⁶ The second of these two sections, i.e., Section 3, treats the same problem, but for a pair of point sources. This gets us into a situation where we could examine isoplanatism effects, but at this point we develop results assuming that the point sources are close enough to each other that there is no anisoplanatism problem. The completion of this analysis prepares all of the background that we need, and in Section 4 we are able to analyze the dual point source problem with a large enough separation between the points that anisoplanatism effects have to be considered. This provides us with the basic isoplanatism results for the Labeyrie technique. In the two sections following this, we switch our attention to the Knox-Thompson concept. In Section 5, we treat a pair of point sources close enough together that there is no anisoplanatism effect. The results presented here parallel the basic work of Knox.⁷ In Section 6, we extend this analysis to allow consideration of the case in which the two point sources are far enough apart that anisoplanatism effects have to be taken into account. In this section, we develop our fundamental results for isoplanatism for the Knox-Thompson concept. Section 7, the final section, reviews all of the results and indicates their significance.

Our approach throughout this paper will be to use a notation that is sufficiently general that it allows treatment of all of the problems. This will permit us to use one self-consistent notation throughout the paper. It will, of course, force us to utilize an overly complex notation in some places, but while this may appear locally inelegant, it will make the totality of the paper easier to read.

Our analysis will be directed to the problem of optical propagation down through the atmosphere, and small to moderate zenith angles. For this case, we may assume that the intensity fluctuation effects, as measured by the log-amplitude variance,⁸ are small compared to the phase fluctuation statistics — small enough to be of negligible significance. Accordingly, we shall base our analysis on a formulation in which there is only a turbulence-induced phase variation at the entrance aperture of the telescope; and no corresponding intensity fluctuation effects. In the same vein of reasoning, we shall associate results obtained in terms of the phase structure function as though they applied to the wave-structure function.⁹ It can be shown that the discrepancy introduced by this approach is of the order of an exponential of the log-amplitude variance,¹⁰ so that it should consequently be quite small for the problem scenario of interest to us here, i. e., astronomical viewing geometry.

2. Labeyrie Technique: Single Point Source

We consider a single point source at an angular position in our field-of-view of $\vec{\theta}_j$. We assume that the source intensity, at wavelength λ , is such that the amplitude at our telescope aperture is A_j . If we denote position on the telescope aperture by the two-dimensional vector \vec{r} , and let $\phi(\vec{\theta}_j; \vec{r})$ denote the instantaneous random phase shift at \vec{r} introduced by atmospheric turbulence, then we can write for the wave function at the telescope aperture due to this point source

$$U_j(\vec{r}) = A_j \exp [ik\vec{\theta}_j \cdot \vec{r} + i\phi(\vec{\theta}_j; \vec{r})] \quad , \quad (1)$$

where

$$k = 2\pi/\lambda \quad , \quad (2)$$

is the optical wave number.

We assume that the telescope has a circular clear aperture with a diameter, D . It is convenient to introduce here the function

$$W(\vec{r}) = \begin{cases} 1 & , \quad \text{if} \quad |\vec{r}| \leq \frac{1}{2} D \\ 0 & , \quad \text{if} \quad |\vec{r}| > \frac{1}{2} D \end{cases} \quad , \quad (3)$$

to provide a mathematical definition of the aperture. Defining position in the telescope plane in terms of the corresponding field-angle, $\vec{\theta}$, the wave function due to our point source as it appears on the focal plane can be written as

$$u_j(\vec{\theta}) = \eta \int d\vec{r} W(\vec{r}) \exp (-ik\vec{\theta} \cdot \vec{r}) U_j(\vec{r}) \quad , \quad (4)$$

where η is a constant of proportionality whose exact value is of no

particular concern to us as it will drop out of our final results.

The focal plane intensity can be written as

$$I(\vec{\theta}) = \frac{1}{2} |u_j(\vec{\theta})|^2 \quad . \quad (5)$$

The quantities of immediate interest to us are the fourier (angular) spatial frequency transform of the focal plane intensity,

$$S(\vec{f}) = \int d\vec{\theta} \exp(-2\pi i \vec{f} \cdot \vec{\theta}) I(\vec{\theta}) \quad , \quad (6)$$

where \vec{f} is the spatial frequency (in units of cycles per radian-field-of-view), and a quantity, $\mathcal{J}(\vec{f}, \vec{f}')$, which we call the bispectrum, and which is defined by the equation

$$\mathcal{J}(\vec{f}, \vec{f}') = \langle S^*(\vec{f}') S(\vec{f}) \rangle \quad . \quad (7)$$

Here and throughout this work we use the angle brackets to denote an ensemble average over all possible realizations of the turbulence-induced wavefront distortion effects. It should be noted that in the case where the two spatial frequencies, \vec{f} and \vec{f}' , are equal, the bispectrum reduces to the ordinary power spectrum. Our notation, i.e., $\mathcal{J}(\vec{f}, \vec{f}')$, allowing for two distinct spatial frequencies is more general than we shall need for analysis of the Labeyrie technique, where \vec{f} and \vec{f}' will always be equal. However, use of this generalized notation will allow a smooth transition of the analytic work into Sections 5 and 6, where we will analyze the Knox-Thompson concept.

It should be noted that we have dropped the subscript, j , from the definition of $I(\vec{f})$, the focal plane power density. This will allow the same notation for focal plane intensity, I , and thus for its transform, S , and the bispectrum, \mathcal{J} , to be used whether we are considering a single point source, (j) , or a pair of point sources, $(j \text{ and } j')$.

If we substitute Eq. (1) into Eq. (4), we get

$$u_j(\vec{\theta}) = u A_j \int d\vec{r} W(\vec{r}) \exp [i\phi(\vec{\theta}_j; \vec{r}) - ik(\vec{\theta} - \vec{\theta}_j) \cdot \vec{r}] \quad (8)$$

Substituting this into Eq. (5), and rewriting the product of integrals as a double integral, we get

$$I(\vec{\theta}) = \frac{1}{2} |u|^2 A_j^2 \iint d\vec{r} d\vec{r}' W(\vec{r}) W(\vec{r}') \times \exp \{i[\phi(\vec{\theta}_j; \vec{r}) - \phi(\vec{\theta}_j; \vec{r}')] - ik[(\vec{\theta} - \vec{\theta}_j) \cdot (\vec{r} - \vec{r}')]\} \quad (9)$$

In accordance with Eq. (6), we can write for the spatial frequency fourier transform

$$S(\vec{f}) = \frac{1}{2} |u|^2 A_j^2 \iiint d\vec{\theta} d\vec{r} d\vec{r}' W(\vec{r}) W(\vec{r}') \times \exp (-2\pi i \vec{f} \cdot \vec{\theta}) \exp \{i[\phi(\vec{\theta}; \vec{r}) - \phi(\vec{\theta}; \vec{r}')] - ik[(\vec{\theta} - \vec{\theta}_j) \cdot (\vec{r} - \vec{r}')]\} \quad (10)$$

Replacing the variable of integration $\vec{\theta}$ by $\vec{\theta} = \vec{\theta} - \vec{\theta}_j$, we get in place of Eq. (10)

$$S(\vec{f}) = \frac{1}{2} |u|^2 A_j^2 \exp (-2\pi i \vec{f} \cdot \vec{\theta}_j) \iiint d\vec{\theta} d\vec{r} d\vec{r}' \times W(\vec{r}) W(\vec{r}') \exp \{i[\phi(\vec{\theta}_j; \vec{r}) - \phi(\vec{\theta}_j; \vec{r}')] - ik\vec{\theta} \cdot (\vec{r} + \lambda \vec{r} - \vec{r}')\} \quad (11)$$

It is a well-known property of the fourier transformation that the repeated fourier integral recovers the starting function. Thus for $h(y)$ being any reasonably well behaved function

$$\iint dx dy' \exp [\pm 2\pi i x (y-y')] h(y) = h(y) \quad (12)$$

Making use of this result, we can perform the \vec{r} - and \vec{r}' -integrations in Eq. (11). Thus we obtain the result that

$$S(\vec{f}) = \frac{1}{2} |u|^2 A_j^2 \exp (-2\pi i \vec{f} \cdot \vec{\theta}_j) \int d\vec{r} W(\vec{r}) W(\vec{r} + \lambda \vec{f}) \\ \times \exp \{i[\phi(\vec{\theta}_j; \vec{r}) - \phi(\vec{\theta}_j; \vec{r} + \lambda \vec{f})]\} \quad (13)$$

where we have suppressed a factor of λ^2 in this result by lumping it in with the constant $|u|^2$.

We calculate the bispectrum, or rather since we are interested in the case where $\vec{f} = \vec{f}'$, the power spectrum $\mathcal{J}(\vec{f}, \vec{f})$, which we will write as

$$\mathcal{J}(\vec{f}) = \mathcal{J}(\vec{f}; \vec{f}) \quad (14)$$

by substituting Eq. (13) into Eq. (7). This gives us the result that

$$\mathcal{J}(\vec{f}) = \frac{1}{2} |u|^4 (A_j^2)^2 \iint d\vec{r} d\vec{r}' W(\vec{r}) W(\vec{r} + \lambda \vec{f}) \\ \times W(\vec{r}') W(\vec{r}' + \lambda \vec{f}) \langle \exp \{i[\phi(\vec{\theta}_j; \vec{r}) - \phi(\vec{\theta}_j; \vec{r}') \\ + \phi(\vec{\theta}_j; \vec{r}' + \lambda \vec{f}) - \phi(\vec{\theta}_j; \vec{r} + \lambda \vec{f})]\} \rangle \quad (15)$$

where, in order to obtain this result, we have made a double integral of the product of integrals.

To reduce this expression, we start by noting that the quantity in the square brackets in the exponential is a gaussian random variable with zero mean, and that for such a random variable, say χ , with α being any constant,

$$\langle \exp(\alpha \chi) \rangle = \exp\left(\frac{1}{2} \alpha^2 \langle \chi^2 \rangle\right) \quad (16)$$

Making use of this result and the fact that

$$(a-b+c-d)^2 = (a-b)^2 - (a-c)^2 + (a-d)^2 + (b-c)^2 - (b-d)^2 + (c-d)^2, \quad (17)$$

we can rewrite Eq. (15) as

$$\begin{aligned} \tilde{J}(\vec{f}) = & \frac{1}{2} |u|^4 (A_s)^2 \iint d\vec{r} d\vec{r}' W(\vec{r}) W(\vec{r} + \lambda \vec{f}) \\ & \times W(\vec{r}') W(\vec{r}' + \lambda \vec{f}) \exp \left\{ -\frac{1}{2} [B(\vec{r} - \vec{r}') \right. \\ & - B(\vec{r} - \vec{r}' - \lambda \vec{f}) + B(\lambda \vec{f}) + B(\lambda \vec{f}) - B(\vec{r} - \vec{r}' + \lambda \vec{f}) \\ & \left. + B(\vec{r} - \vec{r}') \right] \} \end{aligned} \quad (18)$$

where $B(\vec{\rho})$ is the wave-structure function, defined by the equation

$$B(\vec{\rho}) = \langle [\phi(\vec{0}, \vec{r} + \vec{\rho}) - \phi(\vec{0}, \vec{r})]^2 \rangle \quad (19)$$

Consideration of the statistical symmetry of the wave-structure function makes it clear that $B(\vec{\rho}) = B(-\vec{\rho})$, a fact which we have used in developing Eq. (18) in the form presented.

It is obvious that when we consider the zero frequency case, i.e., when $\vec{f} \equiv 0$, the exponential in Eq. (18) goes to $\exp(0) = 1$, so that we can write

$$\tilde{J}(0) = \frac{1}{2} |u|^4 (A_s)^2 \iint d\vec{r} d\vec{r}' [W(\vec{r})]^2 [W(\vec{r}')]^2 \quad (20)$$

Consideration of Eq. (3) makes it apparent that W -squared is equal to W . Moreover, we note that the double integral of Eq. (20) can be rewritten as the product of two identical integrals, each equal to $\frac{1}{4}\pi D^2$. Thus we can rewrite Eq. (20) as

$$\tilde{J}(0) = \left(\frac{\pi}{8} |\psi|^2 A_s^2 D^2 \right)^2 \quad (21)$$

This will provide a basis for normalization of the results we shall develop shortly.

To proceed with the reduction of Eq. (18), we make use of the fact that the wave-structure function can be written as^{11,12}

$$D(\vec{\rho}) = 6.88 (\rho/r_0)^{5/3} \quad (22)$$

where r_0 is a length which serves as a measure of the transverse coherence of the turbulence distorted wavefront. Thus we can rewrite the exponent in Eq. (18) as

$$\begin{aligned} E &= -\frac{1}{2} [D(\vec{r}-\vec{r}') - D(\vec{r}-\vec{r}'-\lambda\vec{f}) + D(\lambda\vec{f}) + D(\lambda\vec{f}) \\ &\quad - D(\vec{r}-\vec{r}'+\lambda\vec{f}) + D(\vec{r}-\vec{r}')] \\ &= -[D(\vec{r}-\vec{r}') + D(\lambda\vec{f}) - \frac{1}{2} D(\vec{r}-\vec{r}'-\lambda\vec{f}) - \frac{1}{2} D(\vec{r}-\vec{r}'+\lambda\vec{f})] \\ &= -6.88 r_0^{-5/3} (|\vec{r}-\vec{r}'|^{5/3} + |\lambda\vec{f}|^{5/3} - \frac{1}{2} |\vec{r}-\vec{r}'-\lambda\vec{f}|^{5/3} \\ &\quad - \frac{1}{2} |\vec{r}-\vec{r}'+\lambda\vec{f}|^{5/3}) \quad (23) \end{aligned}$$

Based on the approximation that

$$\begin{aligned} 1 + \epsilon^{5/3} - \frac{1}{2} (1 + 2\epsilon \cos \theta + \epsilon^2)^{5/3} - \frac{1}{2} (1 - 2\epsilon \cos \theta + \epsilon^2)^{5/3} \\ \approx \epsilon^{5/3} \left[1 - \frac{5}{6} \epsilon^{1/3} (1 - \frac{1}{3} \cos^2 \theta) \right] \quad (24) \end{aligned}$$

which is accurate for small enough values of ϵ , and noting that, by virtue of the law of cosines, we can write

$$|\vec{r}-\vec{r}' \pm \lambda \vec{f}|^{5/3} = (|\vec{r}-\vec{r}'|^2 \pm 2|\vec{r}-\vec{r}'||\lambda \vec{f}| \cos \theta + |\lambda \vec{f}|^2)^{5/3}, \quad (25)$$

where θ is the angle between the vectors $(\vec{r}-\vec{r}')$ and $(\lambda \vec{f})$, we can introduce the approximations that

$$E \approx -6.88 (\lambda |\vec{f}| / r_0)^{5/3} \left[1 - \frac{5}{6} \left(\frac{\lambda |\vec{f}|}{|\vec{r}-\vec{r}'|} \right)^{1/3} (1 - \frac{1}{3} \cos^2 \theta) \right],$$

if $\lambda |\vec{f}| \ll |\vec{r}-\vec{r}'|$, (26)

and

$$E \approx -6.88 (|\vec{r}-\vec{r}'| / r_0)^{5/3} \left[1 - \frac{5}{6} \left(\frac{|\vec{r}-\vec{r}'|}{\lambda |\vec{f}|} \right)^{1/3} (1 - \frac{1}{3} \cos^2 \theta) \right],$$

if $|\vec{r}-\vec{r}'| \ll \lambda |\vec{f}|$. (27)

In developing Eq. (26) from Eq. (23), terms of higher order in $|\lambda \vec{f}| / |\vec{r}-\vec{r}'|$ have been dropped from inside the square brackets. [The first term dropped is proportional to $(\lambda |\vec{f}| / |\vec{r}-\vec{r}'|)^{7/3}$.] Similarly, in developing Eq. (27) from Eq. (23), terms of higher order in $|\vec{r}-\vec{r}'| / |\lambda \vec{f}|$ have been dropped from inside the square brackets on the right hand side of Eq. (27). [Here the first term dropped is proportional to $(|\vec{r}-\vec{r}'| / \lambda |\vec{f}|)^{7/3}$.] For our purposes, it will be sufficient to replace Eq. 's (26) and (27) with the further approximation that

$$E \approx -6.88 (\lambda |\vec{f}| / r_0)^{5/3}, \quad \text{if } \lambda |\vec{f}| \ll |\vec{r}-\vec{r}'|, \quad (28)$$

$$E \approx -6.88 (|\vec{r}-\vec{r}'| / r_0)^{5/3}, \quad \text{if } |\vec{r}-\vec{r}'| \ll \lambda |\vec{f}|. \quad (29)$$

If we study the exponential in Eq. (18) subject to the assumption that $\lambda |\vec{f}|$ is very large compared to r_0 , we see that the only condition

under which the exponential function will not be vanishingly small is when $|\vec{r}-\vec{r}'|$ is not much larger than (or smaller than) r_0 . In this case, in accordance with Eq. (29), we can write

$$\tilde{J}(\vec{r}) \approx \frac{1}{4} |u|^4 (A_j)^2 \iint d\vec{r} d\vec{r}' W(\vec{r}) W(\vec{r}+\lambda\vec{f}) W(\vec{r}') W(\vec{r}'+\lambda\vec{f}) \times \exp [-6.88 (|\vec{r}-\vec{r}'|/r_0)^{5/3}] \quad (30)$$

It will be noted that the double integral in Eq. (30) appears to allow the case where $|\vec{r}-\vec{r}'|$ is not particularly small. Strictly speaking, we should include some condition in the integrand restricting the range of integration so that we only considered pairs of values of (\vec{r}, \vec{r}') for which $|\vec{r}-\vec{r}'|$ was comparable to or smaller than r_0 . In fact, however, such a restriction is automatically provided by the exponential function in Eq. (30).

Based on the assumption that the aperture diameter D is much larger than r_0 , and noting that the form of the exponential makes the integrand vanish when \vec{r} is not nearly equal to \vec{r}' (i.e., when $|\vec{r}-\vec{r}'|$ is not comparable to or smaller than r_0), we can make the approximations that

$$W(\vec{r}) \approx W(\vec{r}') \quad , \quad \text{in Eq. (30)} \quad , \quad (31)$$

$$W(\vec{r}+\lambda\vec{f}) \approx W(\vec{r}'+\lambda\vec{f}) \quad , \quad \text{in Eq. (30)} \quad . \quad (32)$$

In accordance with Eq. (3), we can write

$$W(\vec{r}) W(\vec{r}') \approx W(\vec{r}) \quad , \quad \text{in Eq. (30)} \quad . \quad (33)$$

$$W(\vec{r}+\lambda\vec{f}) W(\vec{r}'+\lambda\vec{f}) \approx W(\vec{r}+\lambda\vec{f}) \quad , \quad \text{in Eq. (30)} \quad . \quad (34)$$

If we make a change of variable of integration in Eq. (30) from (\vec{r}, \vec{r}') to (\vec{r}, \vec{x}) , where

$$\vec{x} = \vec{r} - \vec{r}' \quad (35)$$

then with the use of Eq.'s (33) and (34), we can rewrite Eq. (30) as

$$\begin{aligned} J(\vec{r}) = & \frac{1}{2} |g|^4 \langle A_j^2 \rangle^2 \left\{ \int d\vec{r} W(\vec{r}) W(\vec{r} + \lambda \vec{r}) \right\} \\ & \times \left\{ \int d\vec{x} \exp [-6.88 (|\vec{x}|/r_0)^{5/3}] \right\} \end{aligned} \quad (36)$$

The integral in the second curly brackets can be evaluated by rewriting it in polar coordinates, performing the azimuthal integration, and making a change of variable for the radial integration so as to cast the integral in the form of a gamma-function, $\Gamma(6/5)$ to be exact. Thus it can be shown that

$$\begin{aligned} & \int d\vec{x} \exp [-6.88 (|\vec{x}|/r_0)^{5/3}] \\ &= 2\pi \int_0^\infty x dx \exp [-6.88 (x/r_0)^{5/3}] \\ &= [\pi / (6.88/r_0)^{3/5}] \int_0^\infty du \exp (-u^{5/3}) \\ &= \frac{6}{5} [\pi / (6.88/r_0^{5/3})^{3/5}] \int_0^\infty v^{1/5} dv \exp (-v) \\ &= \frac{6}{5} [\pi / (6.88/r_0^{5/3})^{3/5}] \Gamma(6/5) \\ &= 0.342 r_0^2 \end{aligned} \quad (37)$$

The integral in the first curly brackets in Eq. (36) can be recognized as corresponding to the area of overlap of two circles of diameter D , with center-to-center separation of $\lambda \vec{r}$. This corresponds to the aperture area, $\frac{1}{4} \pi D^2$, times the diffraction-limited optical transfer function,

$$\tau_{0L}(\vec{f}) = \frac{2}{\pi} \{ \cos^{-1}(\lambda|\vec{f}|/D) - (\lambda|\vec{f}|/D) [1 - (\lambda|\vec{f}|/D)^2]^{1/2} \} , \quad (38)$$

for optics of diameter D operating at wavelength λ . Thus Eq. (36) can be rewritten as

$$\tilde{J}(\vec{f}) = \frac{1}{4} |u|^4 (A_j)^2 \{ \frac{1}{4} \pi D^2 \tau_{0L}(\vec{f}) \} \{ 0.342 r_0^2 \} . \quad (39)$$

With a bit of manipulation of terms, and making use of Eq. (21), this result can be rewritten in normalized form, representing the speckle transfer function as

$$\frac{\tilde{J}(\vec{f})}{\tilde{J}(0)} = 0.435 (r_0/D)^2 \tau_{0L}(\vec{f}) , \quad \text{for } \lambda|\vec{f}| \gg r_0 . \quad (40)$$

(It can be shown that 0.435 is actually an approximation for $2^{-6/5} \approx 0.435$.)

If we now study Eq. (18) subject to the assumption that $\lambda|\vec{f}|$ is small compared to r_0 , then we can see that in this case the exponential function will only deviate from unity when $|\vec{r}-\vec{r}'|$ is large enough that the small difference between $\vec{r}-\vec{r}'$ and $\vec{r}-\vec{r}' \pm \lambda\vec{f}$ makes the cancellation of the $B(\vec{r}-\vec{r}')$ and $B(\vec{r}-\vec{r}' \pm \lambda\vec{f})$ -terms significantly inexact. In this case, we may use Eq. (28) to allow us to rewrite Eq. (18) as

$$\begin{aligned} \tilde{J}(\vec{f}) = \frac{1}{4} |u|^4 (A_j)^2 \iint d\vec{r} d\vec{r}' W(\vec{r}) W(\vec{r}+\lambda\vec{f}) W(\vec{r}') W(\vec{r}'+\lambda\vec{f}) \\ \times \exp [-6.88 (\lambda|\vec{f}|/r_0)^{5/3}] . \end{aligned} \quad (41)$$

In this case, the double integral can be decomposed into the produce of two identical integrals, and we can write

$$\begin{aligned} \tilde{J}(\vec{f}) = \left\{ \frac{1}{2} |u|^2 (A_j)^2 \exp [-3.44 (\lambda|\vec{f}|/r_0)^{5/3}] \right. \\ \left. \times \int d\vec{r} W(\vec{r}) W(\vec{r}+\lambda\vec{f}) \right\}^2 , \end{aligned} \quad (42)$$

where, since the exponential is not a function of the variable of integration, we have taken it out of the integral (and then taken its square root, along with that of $\frac{1}{4} |g|^4 (A_j^2)^2$, thus replacing 6.88 by 3.44). The integral can be recognized as the area of overlap of two circles of diameter D with center-to-center separation of $\lambda \vec{f}$. As noted before, this integral can be written as

$$\int d\vec{r} W(\vec{r}) W(\vec{r} + \lambda \vec{f}) = \frac{1}{4} \pi D^2 \tau_{0L}(\vec{f}), \quad (43)$$

where τ_{0L} , as defined by Eq. (38), is the optical transfer function for a circular aperture optical system operating at wavelength λ . Making use of Eq. 's (21) and (43), we can rewrite Eq. (42), in terms of the speckle transfer function as

$$\frac{\tilde{J}(\vec{f})}{\tilde{J}(0)} = \{\tau_{0L}(\vec{f})\}^2 \exp[-6.88 (\lambda |\vec{f}| / r_0)^{5/3}], \text{ for } \lambda |\vec{f}| \ll r_0. \quad (44)$$

Eq. 's (40) and (44), with Eq. (38) supporting, represent our basic results for the analysis of the performance of the Labeyrie technique operating against a single point source—though the fact that these results are applicable to the Labeyrie technique is not immediately apparent from what we have said thus far. We shall discuss this applicability shortly, but before we do this, it is worthwhile to consider the accuracy of the approximations we have made in developing Eq. 's (40) and (44) from Eq. (18) [and Eq. (21)]. This will be of value in our later analysis where we shall want to make the same kind of approximations.

To demonstrate the accuracy of Eq. 's (40) and (44), we have carried out numerical evaluation of the double integral in Eq. (18), and obtained exact results for the speckle transfer function, $\tilde{J}(\vec{f})/\tilde{J}(0)$. The integral evaluations were carried out using Monte Carlo techniques.* In Fig. 's 1 to 5,

* To insure reasonably rapid convergences of our Monte Carlo results, we used uniform sampling over the \vec{r} and \vec{r}' circles when $\lambda |\vec{f}|$ is less than r_0 —but when $\lambda \vec{f}$ is greater than r_0 , we made the variables of integration

(Continued on next page)

we show these results for $D/r_0 = 10, 30, 100, 300, \text{ and } 1000$.

Also shown are the approximate results calculated from Eq. 's (40) and (44). As can be seen, these approximate results are quite accurate in their respective limits—and accordingly, we argue that the approximation technique we used to develop these equations is basically sound. In particular, we argue that our method of inspection of the exponential in Eq. (18) to decide what relationship between $\vec{r}-\vec{r}'$ and $\lambda \vec{r}$ dominated the result, and thus to justify use of either Eq. (28) or Eq. (29), leads to correct results in the limits of $\lambda \vec{r}$ much larger or much smaller than r_0 , and we shall use it in the following analysis.

At this point, we are ready to take up the question of the relationship between the quantity we have been evaluating, i.e., $\mathcal{J}(\vec{f})/\tilde{\mathcal{J}}(0)$, and the performance of the Labeyrie technique for speckle interferometry. In the Labeyrie technique, the image of an object, $I(\vec{r})$, is formed. This is, of course, a randomly distorted short exposure image. The fourier transform of this image, $S(\vec{f})$ is calculated, and is also a random function, as is $I(\vec{r})$. A series of these are generated and represent a randomly sampled set from the ensemble of all possible atmospheric turbulence-induced distortions of the image. Using this set of image samples and the fourier transforms, the Labeyrie technique then forms the (ensemble) average of the square of the transform, $\mathcal{J}(\vec{f}, \vec{f}) = \tilde{\mathcal{J}}(\vec{f})$. This quantity is taken to represent a measure of the source object's power spectrum. To the extent that high spatial frequencies are present in $\tilde{\mathcal{J}}(\vec{f})$, the correlation function which we can obtain from this power spectrum will contain information on the fine details of the object. In this sense, Eq. (40) is critically important since it means that image details will be present at the diffraction limit. The strength

(Continued from previous page) \vec{r} and $\vec{r}-\vec{r}'$. In this case, we used uniform sampling of \vec{r} over its circle, but sampled $\vec{r}-\vec{r}'$ according to the two-dimensional gaussian distribution with probability density $[2\pi(0.207 r_0^2)]^{-1} \times \exp \{ -\frac{1}{2} [|\vec{r}-\vec{r}'|/(0.207 r_0)]^2 \}$ over the infinite $(\vec{r}-\vec{r}')$ -plane. [We note that $\frac{1}{2} (0.207)^{-2/3} \approx 6.88$.]

of these details is attenuated by a factor of $(r_0/D)[\tau_{0L}(\vec{f})]^{-1/2}$ compared to what would be obtained with diffraction-limited images, i. e., in the absence of turbulence effects. But this attenuation factor is not so large as to be intolerable.

Our analysis to this point, paralleling that of Korff³, demonstrates that with the Labeyrie technique, the high spatial frequencies of the image are not attenuated by more than a factor of $(r_0/D)[\tau_{0L}(\vec{f})]^{-1/2}$, and is of great general interest as it shows that the high spatial frequency details are recoverable. However, since our analysis deals with only a single point source, it is unable to accommodate any isoplanatism effects. To incorporate isoplanatism effects in our analysis, we need to consider a source with some spatial extent. The simplest such source is a pair of point sources. In the next section, we shall present an analysis paralleling the one in this section, but for a pair of point sources—with the assumption that there is no anisoplanatism effect. This will then serve as a reference for the analysis in Section 4 of the Labeyrie technique with a pair of point sources and anisoplanatism effects.

3. Labeyrie Technique: Two Point Sources

We shall consider here a pair of point sources with angular positions $\vec{\theta}_j$ and $\vec{\theta}_{j'}$ in our field-of-view, and amplitudes A_j and $A_{j'}$ at the telescope aperture. We associate atmospheric turbulence-induced wavefront distortions, $\phi(\vec{\theta}_j; \vec{r})$ and $\phi(\vec{\theta}_{j'}; \vec{r})$ with the wavefront sensed at \vec{r} due to each point source. Our assumption that in this case there is no anisoplanatism problem can be translated into the requirement that $\phi(\vec{\theta}_j; \vec{r})$ and $\phi(\vec{\theta}_{j'}; \vec{r})$ are virtually equal, but in anticipation of the problem to be treated in Section 4, where there is an anisoplanatism problem, we shall retain the distinct notation for $\phi(\vec{\theta}_j; \vec{r})$ and $\phi(\vec{\theta}_{j'}; \vec{r})$.

We may write for the wave-function at the optics aperture due to these two point sources, in correspondence with Eq. (1),

$$U_j(\vec{r}) \oplus U_{j'}(\vec{r}) = A_j \exp [ik\vec{\theta}_j \cdot \vec{r} + i\phi(\vec{\theta}_j; \vec{r})] \\ \oplus A_{j'} \exp [ik\vec{\theta}_{j'} \cdot \vec{r} + i\phi(\vec{\theta}_{j'}; \vec{r})] \quad . \quad (45)$$

The special notation, \oplus , is used here to indicate a summation, but of an unusual type. Its proper understanding requires that we recall that the wave-function is actually subject to a temporal oscillation at a frequency kc (of the order of 4×10^{15} rad/sec), and that $U_j(\vec{r})$ is just a phasor associated with this oscillation, which we use to take note of the relationship of the phase of the oscillation at two positions, \vec{r} and \vec{r}' , by means of the product $U_j^*(\vec{r}) U_j(\vec{r}')$. Moreover, the oscillation itself is "somewhat erratic," representing black body radiation over some non-negligible spectral bandwidth. Despite this erratic nature, the phasor $U_j(\vec{r})$ nonetheless represents the relationship between the phase at \vec{r} and \vec{r}' . However, there is no correlation between the erratic oscillations of the radiation from the two point sources, denoted by j and j' , which are statistically independent black body radiation sources. Hence there is no well-defined

phase relationship between the two wave-functions, and $U_j(\vec{r})$ and $U_{j'}(\vec{r})$ have no special meaning with respect to each other—their product has no particular meaning, and will vanish on the average. Thus we use our notation \oplus to denote the presence of two statistically independent phasors, with the understanding that the average of the product of the two phasors will vanish.

In parallel with Eq. (4), we can write for the wave-function at the focal plane of the optical system

$$u_j(\vec{\theta}) \oplus u_{j'}(\vec{\theta}) = \eta \int d\vec{r} W(\vec{r}) \exp(-ik\vec{\theta} \cdot \vec{r}) [U_j(\vec{r}) \oplus U_{j'}(\vec{r})] . \quad (46)$$

In parallel with Eq. (5), we write for the focal plane intensity

$$I(\vec{\theta}) = \frac{1}{2} |u_j(\vec{\theta}) \oplus u_{j'}(\vec{\theta})|^2 . \quad (47)$$

In practice, the time required to measure the intensity is so large compared with the inverse of the spectral bandwidth of the black body radiation (even for a very short exposure) that measurement of the intensity provides sufficient averaging that the cross-product $u_j^* u_{j'}$ in Eq. (47) will vanish. Thus we can write in place of Eq. (47)

$$I(\vec{\theta}) = \frac{1}{2} [|u_j(\vec{\theta})|^2 + |u_{j'}(\vec{\theta})|^2] . \quad (48)$$

With $I(\vec{\theta})$ for a pair of point sources written in this form, Eq. 's (6) and (7) remain applicable here.

We can now write in place of Eq. (9)

$$I(\vec{\theta}) = \frac{1}{2} |\eta|^2 \iint d\vec{r} d\vec{r}' W(\vec{r}) W(\vec{r}') \\ \times \{ A_j^2 \exp \{ i [\phi(\vec{\theta}_j; \vec{r}) - \phi(\vec{\theta}_j; \vec{r}')] - ik[(\vec{\theta} - \vec{\theta}_j) \cdot (\vec{r} - \vec{r}')] \} \}$$

$$+ A_{j'}^2 \exp \{i[\phi(\vec{\theta}_{j'}; \vec{r}) - \phi(\vec{\theta}_{j'}; \vec{r}')] - ik[(\vec{\theta} - \vec{\theta}_{j'}) \cdot (\vec{r} - \vec{r}')]\} \} . \quad (49)$$

Substituting this into Eq. (6) and interchanging order of integration as appropriate, we get for the random amplitude at spatial frequency \vec{f} ,

$$\begin{aligned} S(\vec{f}) = & \frac{1}{2} |u|^2 \iiint d\vec{\theta} d\vec{r} d\vec{r}' W(\vec{r}) W(\vec{r}') \exp(-2\pi i \vec{f} \cdot \vec{\theta}) \\ & \times \left\{ A_j^2 \exp \{i[\phi(\vec{\theta}_j; \vec{r}) - \phi(\vec{\theta}_j; \vec{r}')] - ik[(\vec{\theta} - \vec{\theta}_j) \cdot (\vec{r} - \vec{r}')]\} \right. \\ & \left. + A_{j'}^2 \exp \{i[\phi(\vec{\theta}_{j'}; \vec{r}) - \phi(\vec{\theta}_{j'}; \vec{r}')] - ik[(\vec{\theta} - \vec{\theta}_{j'}) \cdot (\vec{r} - \vec{r}')]\} \right\} . \quad (50) \end{aligned}$$

By separating this expression into a sum of integrals and then replacing the variable of integration, $\vec{\theta}$, by $\vec{\delta} = \vec{\theta} - \vec{\theta}_j$ in one of the integrals, and by $\vec{\delta} = \vec{\theta} - \vec{\theta}_{j'}$ in the other integral, and then combining the sum of integrals into a single integral on a sum, we can obtain in place of Eq. (50) the result that

$$\begin{aligned} S(\vec{f}) = & \frac{1}{2} |u|^2 \iiint d\vec{\delta} d\vec{r} d\vec{r}' W(\vec{r}) W(\vec{r}') \\ & \times \left\{ A_j^2 \exp(-2\pi i \vec{f} \cdot \vec{\theta}_j) \exp \{i[\phi(\vec{\theta}_j; \vec{r}) - \phi(\vec{\theta}_j; \vec{r}')] - ik\vec{\delta} \cdot (\vec{r} + \lambda \vec{f} - \vec{r}')\} \right. \\ & \left. + A_{j'}^2 \exp(-2\pi i \vec{f} \cdot \vec{\theta}_{j'}) \exp \{i[\phi(\vec{\theta}_{j'}; \vec{r}) - \phi(\vec{\theta}_{j'}; \vec{r}')] - ik\vec{\delta} \cdot (\vec{r} + \lambda \vec{f} - \vec{r}')\} \right\} \quad (51) \end{aligned}$$

Now, if we make use of Eq. (12), we can perform the $\vec{\delta}$ - and \vec{r}' -integrations. Thus we can write

$$\begin{aligned} S(\vec{f}) = & \frac{1}{2} |u|^2 \int d\vec{r} W(\vec{r}) W(\vec{r} + \lambda \vec{f}) \\ & \times \left\{ A_j^2 \exp(-2\pi i \vec{f} \cdot \vec{\theta}_j) \exp \{i[\phi(\vec{\theta}_j; \vec{r}) - \phi(\vec{\theta}_j; \vec{r} + \lambda \vec{f})]\} \right. \\ & \left. + A_{j'}^2 \exp(-2\pi i \vec{f} \cdot \vec{\theta}_{j'}) \exp \{i[\phi(\vec{\theta}_{j'}; \vec{r}) - \phi(\vec{\theta}_{j'}; \vec{r} + \lambda \vec{f})]\} \right\} . \quad (52) \end{aligned}$$

We recall here that just as ϕ is a turbulence-driven random function, so is $S(\vec{f})$ a random fourier transform amplitude.

The corresponding power spectral density associated with the spatial frequency \vec{f} can be obtained by substituting Eq. (52) into Eq. (7). Making use of the notation simplification introduced by Eq. (14), making a double integral of the product of integrals, and interchanging the order of ensemble averaging and integration, we write

$$\begin{aligned} \tilde{J}(\vec{f}) = & \frac{1}{4} |u|^4 \iint d\vec{r} d\vec{r}' W(\vec{r}) W(\vec{r} + \lambda \vec{f}) W(\vec{r}') W(\vec{r}' + \lambda \vec{f}) \\ & \times \langle (A_j)^2 \exp \{ i [\phi(\vec{\theta}_j; \vec{r}) - \phi(\vec{\theta}_j; \vec{r} + \lambda \vec{f}) + \phi(\vec{\theta}_j; \vec{r}' + \lambda \vec{f}) - \phi(\vec{\theta}_j; \vec{r}')] \} \\ & + (A_j)^2 (A_{j'})^2 \exp [-2\pi i \vec{f} \cdot (\vec{\theta}_j - \vec{\theta}_{j'})] \\ & \times \exp \{ i [\phi(\vec{\theta}_j; \vec{r}) - \phi(\vec{\theta}_j; \vec{r} + \lambda \vec{f}) + \phi(\vec{\theta}_{j'}; \vec{r}' + \lambda \vec{f}) - \phi(\vec{\theta}_{j'}; \vec{r}')] \} \\ & + (A_j)^2 (A_{j'})^2 \exp [2\pi i \vec{f} \cdot (\vec{\theta}_j - \vec{\theta}_{j'})] \\ & \times \exp \{ -i [\phi(\vec{\theta}_j; \vec{r}) - \phi(\vec{\theta}_j; \vec{r} + \lambda \vec{f}) + \phi(\vec{\theta}_{j'}; \vec{r}' + \lambda \vec{f}) - \phi(\vec{\theta}_{j'}; \vec{r}')] \} \\ & + (A_{j'})^2 \exp \{ i [\phi(\vec{\theta}_{j'}; \vec{r}') - \phi(\vec{\theta}_{j'}; \vec{r}' + \lambda \vec{f}) + \phi(\vec{\theta}_j; \vec{r} + \lambda \vec{f}) - \phi(\vec{\theta}_j; \vec{r})] \} \rangle. \quad (53) \end{aligned}$$

It is to be noted that at this point we have retained terms corresponding to "interference" between the two point sources—but in this case, it is "interference" of the two random intensity patterns.

The ensemble average of the sum of four terms in Eq. (53) can be replaced by the sum of four ensemble averages. Following the procedure used to get from Eq. (15) to Eq. (18), i.e., making use of Eq.'s (16) and (17), and the definition in Eq. (19), we can show that the first and last of the ensemble averages can be reduced to the form

$$\begin{aligned}
& \langle \exp \{ i [\phi(\vec{\theta}_j; \vec{r}) - \phi(\vec{\theta}_j; \vec{r} + \lambda \vec{f}) + \phi(\vec{\theta}_j; \vec{r}' + \lambda \vec{f}) - \phi(\vec{\theta}_j; \vec{r}')]] \} \rangle \\
& = \exp \left(- \{ \mathcal{B}(\vec{r} - \vec{r}') + \mathcal{B}(\lambda \vec{f}) - \frac{1}{2} [\mathcal{B}(\vec{r} - \vec{r}' - \lambda \vec{f}) + \mathcal{B}(\vec{r} - \vec{r}' + \lambda \vec{f})] \} \right) , \quad (54)
\end{aligned}$$

for the first, and similarly for the fourth

$$\begin{aligned}
& \langle \exp \{ i [\phi(\vec{\theta}_{j,\mu}; \vec{r}) - \phi(\vec{\theta}_{j,\mu}; \vec{r} + \lambda \vec{f}) + \phi(\vec{\theta}_{j,\mu}; \vec{r}' + \lambda \vec{f}) - \phi(\vec{\theta}_{j,\mu}; \vec{r}')]] \} \rangle \\
& = \exp \left(- \{ \mathcal{B}(\vec{r} - \vec{r}') + \mathcal{B}(\lambda \vec{f}) - \frac{1}{2} [\mathcal{B}(\vec{r} - \vec{r}' - \lambda \vec{f}) + \mathcal{B}(\vec{r} - \vec{r}' + \lambda \vec{f})] \} \right) . \quad (55)
\end{aligned}$$

Here the results are essentially identical, since, in accordance with Eq. (19), the wave-structure function does not depend on the distinction between $\vec{\theta}_j$ and $\vec{\theta}_{j,\mu}$.

For the reduction of the second and third ensemble averages obtainable from Eq. (53), the procedure is more complex. For example, for the second of the ensemble averages, in accordance with Eq. (16), we would be concerned with

$$\begin{aligned}
& \langle \{ [\phi(\vec{\theta}_j; \vec{r}) - \phi(\vec{\theta}_j; \vec{r} + \lambda \vec{f})] - [\phi(\vec{\theta}_{j,\mu}; \vec{r}') - \phi(\vec{\theta}_{j,\mu}; \vec{r}' + \lambda \vec{f})] \}^2 \rangle \\
& = \langle [\phi(\vec{\theta}_j; \vec{r}) - \phi(\vec{\theta}_j; \vec{r} + \lambda \vec{f})]^2 \rangle + \langle [\phi(\vec{\theta}_{j,\mu}; \vec{r}') - \phi(\vec{\theta}_{j,\mu}; \vec{r}' + \lambda \vec{f})]^2 \rangle \\
& \quad - 2 \langle [\phi(\vec{\theta}_j; \vec{r}) - \phi(\vec{\theta}_j; \vec{r} + \lambda \vec{f})][\phi(\vec{\theta}_{j,\mu}; \vec{r}') - \phi(\vec{\theta}_{j,\mu}; \vec{r}' + \lambda \vec{f})] \rangle \\
& = 2 \mathcal{B}(\lambda \vec{f}) - 2 \langle [\phi(\vec{\theta}_j; \vec{r}) - \phi(\vec{\theta}_j; \vec{r} + \lambda \vec{f})][\phi(\vec{\theta}_{j,\mu}; \vec{r}') - \phi(\vec{\theta}_{j,\mu}; \vec{r}' + \lambda \vec{f})] \rangle . \quad (56)
\end{aligned}$$

Here we have made use of Eq. (19), but replaced $-\lambda \vec{f}$ by $\lambda \vec{f}$, based on the fact implicit in Eq. (22) that the wave-structure function is only dependent on the magnitude of its vector argument. With a bit more algebraic manipulation, Eq. (56) can be rewritten as

$$\begin{aligned}
& \langle [\phi(\bar{\theta}_j; \vec{r}) - \phi(\bar{\theta}_j; \vec{r} + \lambda \vec{f})] - [\phi(\bar{\theta}_{j'}; \vec{r}') - \phi(\bar{\theta}_{j'}; \vec{r}' + \lambda \vec{f})] \rangle^2 \rangle \\
& = 2\mathcal{D}(\lambda \vec{f}) + \langle [\phi(\bar{\theta}_j; \vec{r}) - \phi(\bar{\theta}_{j'}; \vec{r}')]^2 \rangle - \langle [\phi(\bar{\theta}_j; \vec{r}) - \phi(\bar{\theta}_{j'}; \vec{r}' + \lambda \vec{f})]^2 \rangle \\
& \quad - \langle [\phi(\bar{\theta}_j; \vec{r} + \lambda \vec{f}) - \phi(\bar{\theta}_{j'}; \vec{r}')]^2 \rangle + \langle [\phi(\bar{\theta}_j; \vec{r} + \lambda \vec{f}) - \phi(\bar{\theta}_{j'}; \vec{r}' + \lambda \vec{f})]^2 \rangle. \quad (57)
\end{aligned}$$

At this point, making use of Eq. (16) to provide a basis for our use of Eq. (57) in the evaluation of Eq. (53), and substituting Eq. 's (54) and (55) into Eq. (53), we get

$$\begin{aligned}
\mathcal{J}(\vec{f}) &= \frac{1}{4} |\mathcal{W}|^4 \iint d\vec{r} d\vec{r}' W(\vec{r}) W(\vec{r} + \lambda \vec{f}) W(\vec{r}') W(\vec{r}' + \lambda \vec{f}) \\
&\quad \times \left\{ [(A_j)^2 + (A_{j'})^2] \exp \left(-\{\mathcal{D}(\vec{r} - \vec{r}') + \mathcal{D}(\lambda \vec{f}) - \frac{1}{2}[\mathcal{D}(\vec{r} - \vec{r}' - \lambda \vec{f}) \right. \right. \\
&\quad \left. \left. + \mathcal{D}(\vec{r} - \vec{r}' + \lambda \vec{f})]\} \right) \right. \\
&\quad + 2(A_j)^2(A_{j'})^2 \cos [2\pi \vec{f} \cdot (\bar{\theta}_j - \bar{\theta}_{j'})] \exp \{-\mathcal{D}(\lambda \vec{f})\} \\
&\quad - \frac{1}{2} \langle [\phi(\bar{\theta}_j; \vec{r}) - \phi(\bar{\theta}_{j'}; \vec{r}')]^2 \rangle - \frac{1}{2} \langle [\phi(\bar{\theta}_j; \vec{r} + \lambda \vec{f}) - \phi(\bar{\theta}_{j'}; \vec{r}' + \lambda \vec{f})]^2 \rangle \\
&\quad \left. + \frac{1}{2} \langle [\phi(\bar{\theta}_j; \vec{r}) - \phi(\bar{\theta}_{j'}; \vec{r}' + \lambda \vec{f})]^2 \rangle + \frac{1}{2} \langle [\phi(\bar{\theta}_j; \vec{r} + \lambda \vec{f}) - \phi(\bar{\theta}_{j'}; \vec{r}')]^2 \rangle \right\}. \quad (58)
\end{aligned}$$

We first of all note here that by virtue of the stationarity of the wavefront distortion statistics

$$\langle [\phi(\bar{\theta}_j; \vec{r}) - \phi(\bar{\theta}_{j'}; \vec{r}')]^2 \rangle = \langle [\phi(\bar{\theta}_j; \vec{r} + \lambda \vec{f}) - \phi(\bar{\theta}_{j'}; \vec{r}' + \lambda \vec{f})]^2 \rangle. \quad (59)$$

At this point, we introduce the approximation that we can replace $\langle [\phi(\bar{\theta}_j; \vec{r}) - \phi(\bar{\theta}_{j'}; \vec{r}')]^2 \rangle$ by $\langle [\phi(\bar{\theta}_j; \vec{r}') - \phi(\bar{\theta}_{j'}; \vec{r})]^2 \rangle$. This approximation should be quite accurate when $\bar{\theta}_j - \bar{\theta}_{j'}$ is very small (as it always is in cases of interest to us, and particularly accurate within the integral where all values of (\vec{r}, \vec{r}') are considered. With this approximation, and making use of Eq. (59), we can rewrite Eq. (58) as

$$\begin{aligned}
J(\vec{f}) = & \frac{1}{4} |u|^4 \iint d\vec{r} d\vec{r}' W(\vec{r}) W(\vec{r}+\lambda\vec{f}) W(\vec{r}') W(\vec{r}'+\lambda\vec{f}) \\
& \times \left\{ \left[(A_j^2)^2 + (A_{j'}^2)^2 \right] \exp \left(- \{ \mathcal{B}(\vec{r}-\vec{r}') + \mathcal{B}(\lambda\vec{f}) - \frac{1}{2} [\mathcal{B}(\vec{r}-\vec{r}'-\lambda\vec{f}) \right. \right. \\
& \quad \left. \left. + \mathcal{B}(\vec{r}-\vec{r}'+\lambda\vec{f}) \right] \right\} + 2(A_j^2)(A_{j'}^2) \cos [2\pi\vec{f} \cdot (\vec{\theta}_j - \vec{\theta}_{j'})] \exp \{ -\mathcal{B}(\lambda\vec{f}) \\
& \quad - \frac{1}{2} \langle [\phi(\vec{\theta}_j; \vec{r}) - \phi(\vec{\theta}_{j'}; \vec{r}')]^2 \rangle - \frac{1}{2} \langle [\phi(\vec{\theta}_j; \vec{r}') - \phi(\vec{\theta}_{j'}; \vec{r})]^2 \rangle \\
& \quad + \frac{1}{2} \langle [\phi(\vec{\theta}_j; \vec{r}) - \phi(\vec{\theta}_{j'}; \vec{r}'+\lambda\vec{f})]^2 \rangle + \frac{1}{2} \langle [\phi(\vec{\theta}_j; \vec{r}') - \phi(\vec{\theta}_{j'}; \vec{r}+\lambda\vec{f})]^2 \rangle \\
& \quad + \frac{1}{2} \langle [\phi(\vec{\theta}_j; \vec{r}+\lambda\vec{f}) - \phi(\vec{\theta}_{j'}; \vec{r}')]^2 \rangle + \frac{1}{2} \langle [\phi(\vec{\theta}_j; \vec{r}'+\lambda\vec{f}) - \phi(\vec{\theta}_{j'}; \vec{r})]^2 \rangle \} \Big\}
\end{aligned} \tag{60}$$

We have been careful up to this point to retain the distinction between $\phi(\vec{\theta}_j; \vec{x})$ and $\phi(\vec{\theta}_{j'}; \vec{x})$ in our notation. This will make Eq. (60) a valid starting point for our analysis in the next section, when we wish to consider the effects of anisoplanatism. But in this section, we are restricting our attention to the case where $\vec{\theta}_j$ and $\vec{\theta}_{j'}$ are sufficiently close together that we can assume that isoplanatism conditions are satisfied. In this case, we can write for the wave-structure function, in place of Eq. (19),

$$\mathcal{B}(\vec{\rho}) \approx \langle [\phi(\vec{\theta}_j; \vec{r}+\vec{\rho}) - \phi(\vec{\theta}_{j'}; \vec{r})]^2 \rangle \tag{61}$$

Making use of Eq. (61) and of the fact that, in accordance with Eq. (22),

$$\mathcal{B}(\vec{\rho}) = \mathcal{B}(-\vec{\rho}) \tag{62}$$

we can rewrite Eq. (60) as

$$\begin{aligned}
J(\vec{f}) = & \frac{1}{4} |u|^4 \iint d\vec{r} d\vec{r}' W(\vec{r}) W(\vec{r}+\lambda\vec{f}) W(\vec{r}') W(\vec{r}'+\lambda\vec{f}) \\
& \times \left\{ \left[(A_j^2)^2 + (A_{j'}^2)^2 \right] \exp \left(- \{ \mathcal{B}(\vec{r}-\vec{r}') + \mathcal{B}(\lambda\vec{f}) - \frac{1}{2} [\mathcal{B}(\vec{r}-\vec{r}'-\lambda\vec{f}) \right. \right. \\
& \quad \left. \left. + \mathcal{B}(\vec{r}-\vec{r}'+\lambda\vec{f}) \right] \right\} + 2(A_j^2)(A_{j'}^2) \cos [2\pi\vec{f} \cdot (\vec{\theta}_j - \vec{\theta}_{j'})]
\end{aligned}$$

$$\begin{aligned}
& \times \exp \left(- \{ \mathcal{D}(\lambda \vec{f}) + \mathcal{D}(\vec{r} - \vec{r}') - \frac{1}{2} [\mathcal{D}(\vec{r} - \vec{r}' - \lambda \vec{f}) + \mathcal{D}(\vec{r} - \vec{r}' + \lambda \vec{f})] \} \right) \Big\} \\
& = \frac{1}{4} |\mathcal{W}|^4 \{ (A_{j,2})^2 + 2(A_{j,2})(A_{j,2})^2 \cos [2\pi \vec{f} \cdot (\vec{\theta}_j - \vec{\theta}_{j,2})] + (A_{j,2})^2 \} \\
& \times \iint d\vec{r} d\vec{r}' W(\vec{r}) W(\vec{r} + \lambda \vec{f}) W(\vec{r}') W(\vec{r}' + \lambda \vec{f}) \\
& \times \exp \left(- \{ \mathcal{D}(\vec{r} - \vec{r}') + \mathcal{D}(\lambda \vec{f}) - \frac{1}{2} [\mathcal{D}(\vec{r} - \vec{r}' - \lambda \vec{f}) + \mathcal{D}(\vec{r} - \vec{r}' + \lambda \vec{f})] \} \right) . \quad (63)
\end{aligned}$$

At this point, we note that this expression is identical to the one we had to evaluate in the preceding section for the single point source case, as can be seen by comparing Eq. 's (63) and (18). Only the coefficient $(A_{j,2})^2$ in Eq. (18) has been replaced by the more complicated expression $\{ (A_{j,2})^2 + 2(A_{j,2})(A_{j,2})^2 \cos [2\pi \vec{f} \cdot (\vec{\theta}_j - \vec{\theta}_{j,2})] + (A_{j,2})^2 \}$, but this is simply the difference in the spatial frequency power spectra of the single point source and of the pair of point sources. The effect of atmospheric turbulence on the ability of the Labeyrie technique to obtain information on the high spatial frequency part of the image power spectrum is the same, whether the object is a single point source or a pair of point sources, provided that the point sources are close enough together that isoplanatism applies. For the low spatial frequencies, for an isoplanatic pair of point sources, the normalized image spatial frequency power spectrum obtained by the Labeyrie technique can be inferred from Eq. (44) to have the form

$$\begin{aligned}
\frac{\mathcal{J}(\vec{f})}{\mathcal{J}(0)} &= \frac{(A_{j,2})^2 + 2(A_{j,2})(A_{j,2})^2 \cos [2\pi \vec{f} \cdot (\vec{\theta}_j - \vec{\theta}_{j,2})] + (A_{j,2})^2}{[(A_{j,2}) + (A_{j,2})^2]^2} \{ \tau_{0L}(\vec{f}) \}^2 \\
&\text{for } \lambda |\vec{f}| \ll r_0 . \quad (64)
\end{aligned}$$

For high spatial frequencies, we can see from consideration of Eq. (40) that the normalized image spatial frequency power spectrum obtained by the Labeyrie technique has the form

$$\frac{J(\vec{f})}{J(0)} = \frac{(A_{j,0})^2 + 2(A_{j,0})(A_{j,\theta}) \cos [2\pi \vec{f} \cdot (\vec{\theta}_0, -\vec{\theta}_{j,\theta})] + (A_{j,\theta})^2}{[(A_{j,0})^2 + (A_{j,\theta})^2]} \left\{ 0.435 \left(\frac{r_0}{D} \right)^2 \tau_{bl}(\vec{f}) \right\}^2$$

$$\text{for } \lambda |\vec{f}| \gg r_0 \quad . \quad (65)$$

With these results in hand, and Eq. (60) available for future use, we are now ready to turn our attention to the evaluation of atmospheric turbulence effects on the performance of the Labeyrie technique in the absence of isoplanatism. In the next section, we take this up for the case of a pair of point sources.

4. Labeyrie Technique: Anisoplanatism

Our starting point for the evaluation of the effect of anisoplanatism on the Labeyrie technique is Eq. (60), which represents the spatial frequency power spectral density for a pair of point sources. As we recall, in Eq. (60) we retained, but in unreduced form, the distinction between effects of the two point source directions, $\vec{\theta}_j$ and $\vec{\theta}_j'$, on the random phase shifts, $\phi(\vec{\theta}_j; \vec{x})$ and $\phi(\vec{\theta}_j'; \vec{x})$. At this point we return to Eq. (60) but with the objective of developing statistical results showing the dependence of the power spectral density on the angular separation, $\vec{\theta}_j - \vec{\theta}_j'$.

We shall aim our algebraic manipulation of the terms in Eq. (60) at the objective of obtaining results which can make use of a statistical function which we shall call the hyper wave-structure function, and which we define as

$$\begin{aligned} \mathfrak{D}(\vec{\theta}, \vec{\rho}) = & \langle [\phi(\vec{\theta} + \vec{\theta}; \vec{r} + \vec{\rho}) - \phi(\vec{\theta} + \vec{\theta}; \vec{r})] \\ & \times [\phi(\vec{\theta}; \vec{r} + \vec{\rho}) - \phi(\vec{\theta}; \vec{r})] \rangle. \end{aligned} \quad (66)$$

This quantity has previously been studied¹³ and shown to be expressible in terms of an integral over the propagation path. It can be written as

$$\begin{aligned} \mathfrak{D}(\vec{\theta}, \vec{\rho}) = & 8.16 \left(\frac{k}{2\pi} \right)^2 \int_{\text{PATH}} dv C_N^2 \int d\vec{\kappa} [1 - \exp(i\vec{\kappa} \cdot \vec{\rho})] \\ & \times \kappa^{-11/3} [\exp(i\vec{\kappa} \cdot \vec{\theta} v) + \exp(-i\vec{\kappa} \cdot \vec{\theta} v)], \end{aligned} \quad (67)$$

where \vec{x} is a two-dimensional (spatial frequency) vector, and v is a variable of integration measuring position along the propagation path, with $v = 0$ at the plane of the optics aperture, where we "measure" the wavefront distortion statistics. C_N^2 is the so called refractive-index structure constant and is a measure of the local optical strength of the atmospheric turbulence.

Our problem at this point reduces to that of casting the six terms still explicitly in ensemble average form in Eq. (60) into forms that can be identified with Eq. (66). The procedure is tedious but because of its ultimate importance, is worth presenting in detail here. Starting with the expression of interest in Eq. (60), we proceed as follows,

$$\begin{aligned}
& -\frac{1}{2} \langle [\phi(\vec{\theta}_j; \vec{r}) - \phi(\vec{\theta}_j'; \vec{r}')]^2 \rangle - \frac{1}{2} \langle [\phi(\vec{\theta}_j; \vec{r}') - \phi(\vec{\theta}_j'; \vec{r})]^2 \rangle \\
& + \frac{1}{4} \langle [\phi(\vec{\theta}_j; \vec{r}) - \phi(\vec{\theta}_j'; \vec{r}' + \lambda \vec{f})]^2 \rangle + \frac{1}{4} \langle [\phi(\vec{\theta}_j; \vec{r}) - \phi(\vec{\theta}_j'; \vec{r} + \lambda \vec{f})]^2 \rangle \\
& + \frac{1}{4} \langle [\phi(\vec{\theta}_j; \vec{r} + \lambda \vec{f}) - \phi(\vec{\theta}_j'; \vec{r}')]^2 \rangle + \frac{1}{4} \langle [\phi(\vec{\theta}_j; \vec{r}' + \lambda \vec{f}) - \phi(\vec{\theta}_j'; \vec{r})]^2 \rangle \\
& = \langle \phi(\vec{\theta}_j; \vec{r}) \phi(\vec{\theta}_j'; \vec{r}') \rangle + \langle \phi(\vec{\theta}_j; \vec{r}') \phi(\vec{\theta}_j'; \vec{r}) \rangle \\
& - \frac{1}{2} \langle \phi(\vec{\theta}_j; \vec{r}) \phi(\vec{\theta}_j'; \vec{r}' + \lambda \vec{f}) \rangle - \frac{1}{2} \langle \phi(\vec{\theta}_j; \vec{r}') \phi(\vec{\theta}_j'; \vec{r} + \lambda \vec{f}) \rangle \\
& - \frac{1}{2} \langle \phi(\vec{\theta}_j; \vec{r} + \lambda \vec{f}) \phi(\vec{\theta}_j'; \vec{r}') \rangle - \frac{1}{2} \langle \phi(\vec{\theta}_j; \vec{r}' + \lambda \vec{f}) \phi(\vec{\theta}_j'; \vec{r}) \rangle. \quad (68)
\end{aligned}$$

In obtaining the final form of Eq. (68) we have made use of the fact that the wavefront distortion statistics are stationary so that the mean square value of the phase shift, $\langle [\phi(\vec{\theta}; \vec{x})]^2 \rangle$, is the same no matter what the values of $\vec{\theta}$ and \vec{x} . As a consequence all of the mean square phase terms, when summed exactly vanish. Proceeding in the same way we

can show that

$$\begin{aligned}
& - \langle [\phi(\vec{\theta}_j; \vec{r}) - \phi(\vec{\theta}_j; \vec{r}')] [\phi(\vec{\theta}_j'; \vec{r}) - \phi(\vec{\theta}_j'; \vec{r}')] \rangle \\
& + \frac{1}{2} \langle [\phi(\vec{\theta}_j; \vec{r}) - \phi(\vec{\theta}_j; \vec{r} + \lambda \vec{f})] [\phi(\vec{\theta}_j'; \vec{r}) - \phi(\vec{\theta}_j'; \vec{r} + \lambda \vec{f})] \rangle \\
& + \frac{1}{2} \langle [\phi(\vec{\theta}_j; \vec{r}') - \phi(\vec{\theta}_j; \vec{r} + \lambda \vec{f})] [\phi(\vec{\theta}_j'; \vec{r}') - \phi(\vec{\theta}_j'; \vec{r} + \lambda \vec{f})] \rangle \\
& = \langle \phi(\vec{\theta}_j; \vec{r}) \phi(\vec{\theta}_j'; \vec{r}') \rangle + \langle \phi(\vec{\theta}_j; \vec{r}') \phi(\vec{\theta}_j'; \vec{r}) \rangle \\
& - \frac{1}{2} \langle \phi(\vec{\theta}_j; \vec{r}) \phi(\vec{\theta}_j'; \vec{r}' + \lambda \vec{f}) \rangle - \frac{1}{2} \langle \phi(\vec{\theta}_j; \vec{r}' + \lambda \vec{f}) \phi(\vec{\theta}_j'; \vec{r}) \rangle \\
& - \frac{1}{2} \langle \phi(\vec{\theta}_j; \vec{r}') \phi(\vec{\theta}_j'; \vec{r} + \lambda \vec{f}) \rangle - \frac{1}{2} \langle \phi(\vec{\theta}_j; \vec{r} + \lambda \vec{f}) \phi(\vec{\theta}_j'; \vec{r}') \rangle. \quad (69)
\end{aligned}$$

In developing the final form of Eq. (69) we have again made use of the statistical stationarity of the random wavefront distortion. This allows us to argue that the value of $\langle \phi(\vec{\theta}_j; \vec{x}) \phi(\vec{\theta}_j'; \vec{x}) \rangle$ is independent of \vec{x} . This in turn, results in the summing to zero of the several terms of this form that would otherwise appear in the final form of Eq. (69).

It now follows directly from comparison of the final forms of Eq. 's (68) and (69) that the two starting forms are equal. The starting form of Eq. (68) represents a part of the exponent in Eq. (60), while the starting form of Eq. (69) can be seen, from consideration of Eq. (66), to correspond to the sum of several hyper wave-structure functions. Thus we can rewrite Eq. (60) as

$$\tilde{J}(\vec{f}) = \frac{1}{4} |u|^4 \iint d\vec{r} d\vec{r}' W(\vec{r}) W(\vec{r} + \lambda \vec{f}) W(\vec{r}') W(\vec{r}' + \lambda \vec{f})$$

$$\begin{aligned}
& \times \left\{ [(A_j^2)^2 + (A_{j'}^2)^2] \exp \left(-\{ \mathcal{D}(\vec{r} - \vec{r}') + \mathcal{D}(\lambda \vec{f}) - \frac{1}{2} [\mathcal{D}(\vec{r} - \vec{r}' - \lambda \vec{f}) + \mathcal{D}(\vec{r} - \vec{r}' + \lambda \vec{f})] \} \right) \right. \\
& + 2(A_j^2)(A_{j'}^2) \cos [2\pi \vec{f} \cdot (\vec{\theta}_j - \vec{\theta}_{j'})] \exp \left(-\{ \mathcal{D}(\vec{\theta}_j - \vec{\theta}_{j'}, \vec{r} - \vec{r}') + \mathcal{D}(\lambda \vec{f}) \right. \\
& \left. \left. - \frac{1}{2} [\mathcal{D}(\vec{\theta}_j - \vec{\theta}_{j'}, \vec{r} - \vec{r}' - \lambda \vec{f}) + \mathcal{D}(\vec{\theta}_j - \vec{\theta}_{j'}, \vec{r} - \vec{r}' + \lambda \vec{f})] \} \right) \right\}. \quad (70)
\end{aligned}$$

Examination of Eq. (67) will show that the hyper wave-structure function possesses sufficient symmetry that

$$\mathcal{D}(\vec{\theta}, \vec{\rho}) = \mathcal{D}(\vec{\theta}, -\vec{\rho}) \quad (71)$$

This allows us to rewrite Eq. (70) in the form

$$\begin{aligned}
\tilde{W}(\vec{f}) &= \frac{1}{4} |\mathcal{W}|^4 \iint d\vec{r} d\vec{r}' W(\vec{r}) W(\vec{r} + \lambda \vec{f}) W(\vec{r}') W(\vec{r} + \lambda \vec{f}) \\
& \times \left\{ [(A_j^2) + (A_{j'}^2)]^2 \exp \left(-\{ \mathcal{D}(\vec{r} - \vec{r}') + \mathcal{D}(\lambda \vec{f}) - \frac{1}{2} [\mathcal{D}(\vec{r} - \vec{r}' - \lambda \vec{f}) + \mathcal{D}(\vec{r} - \vec{r}' + \lambda \vec{f})] \} \right) \right. \\
& + 2(A_j^2)(A_{j'}^2) \cos [2\pi \vec{f} \cdot (\vec{\theta}_j - \vec{\theta}_{j'})] \\
& \times \exp \left(-\{ \mathcal{D}(\vec{\theta}_j - \vec{\theta}_{j'}, \vec{r} - \vec{r}') + \mathcal{D}(\lambda \vec{f}) - \frac{1}{2} [\mathcal{D}(\vec{\theta}_j - \vec{\theta}_{j'}, \vec{r} - \vec{r}' - \lambda \vec{f}) \right. \\
& \left. \left. + \mathcal{D}(\vec{\theta}_j - \vec{\theta}_{j'}, \vec{r} - \vec{r}' + \lambda \vec{f})] \} \right) \right\}. \quad (72)
\end{aligned}$$

To isolate the field-angle dependence we rewrite this as

$$\begin{aligned}
\tilde{J}(\vec{f}) = & \frac{1}{4} |u|^4 \iint d\vec{r} d\vec{r}' W(\vec{r}) W(\vec{r} + \lambda\vec{f}) W(\vec{r}') W(\vec{r}' + \lambda\vec{f}) \\
& \times \left\{ \left[(A_j^2)^2 + (A_{j'}^2)^2 \right] \exp \left(- \{ \mathcal{D}(\vec{r} - \vec{r}') + \mathcal{D}(\lambda\vec{f}) - \frac{1}{2} [\mathcal{D}(\vec{r} - \vec{r}' - \lambda\vec{f}) + \mathcal{D}(\vec{r} - \vec{r}' + \lambda\vec{f})] \} \right) \right. \\
& + 2(A_j^2)(A_{j'}^2) \cos[2\pi\vec{f} \cdot (\vec{\theta}_j - \vec{\theta}_{j'})] \\
& \left. \times \exp \left(- \{ \mathcal{D}(\vec{r} - \vec{r}') + \mathcal{D}(\lambda\vec{f}) - \frac{1}{2} [\mathcal{D}(\vec{r} - \vec{r}' - \lambda\vec{f}) + \mathcal{D}(\vec{r} - \vec{r}' + \lambda\vec{f})] \} + Q(\vec{\theta}_j - \vec{\theta}_{j'}, \vec{r} - \vec{r}', \lambda\vec{f}) \right) \right\}, \quad (73)
\end{aligned}$$

where

$$\begin{aligned}
Q(\vec{\theta}_j - \vec{\theta}_{j'}, \vec{r} - \vec{r}', \lambda\vec{f}) = & \{ [\mathcal{D}(\vec{r} - \vec{r}') - \mathcal{D}(\vec{\theta}_j - \vec{\theta}_{j'}, \vec{r} - \vec{r}')] \\
& - \frac{1}{2} [\mathcal{D}(\vec{r} - \vec{r}' - \lambda\vec{f}) - \mathcal{D}(\vec{\theta}_j - \vec{\theta}_{j'}, \vec{r} - \vec{r}' - \lambda\vec{f})] \\
& - \frac{1}{2} [\mathcal{D}(\vec{r} - \vec{r}' + \lambda\vec{f}) - \mathcal{D}(\vec{\theta}_j - \vec{\theta}_{j'}, \vec{r} - \vec{r}' + \lambda\vec{f})] \}. \quad (74)
\end{aligned}$$

It is obvious that when Q equals zero $\tilde{J}(\vec{f})$ is identical to what we computed in the previous section, when there was no anisoplanatism effect. It can be seen from a comparison of the definitions of the wave-structure function, \mathcal{D} , and the hyper wave-structure function, \mathcal{D} , as provided by Eq. 's (19) and (66) respectively, that when $\vec{\theta}_j - \vec{\theta}_{j'}$ is equal to zero Q will vanish and there will be no isoplanatism problem. The question we address ourselves to is how large $\vec{\theta}_j - \vec{\theta}_{j'}$ can be before we encounter anisoplanatism problems, i. e., before Q becomes comparable to or larger than minus one.

We recall from our analysis in the previous two sections that when we are interested in large values of $\lambda|\vec{f}|$, i. e., in the high spatial frequencies the value of the double integral defining the power spectral

density, $\tilde{\rho}$, is determined by the region of (\vec{r}, \vec{r}') space where $|\vec{r} - \vec{r}'|$ is much less than $\lambda|\vec{f}|$. Accordingly, we restrict our investigation of the relationship between the value of $\vec{\theta}_j - \vec{\theta}_{j'}$ and anisoplanatism to the case where $\lambda|\vec{f}|$ is much larger than r_0 , i.e., to high spatial frequencies, and where $|\vec{r} - \vec{r}'|$ is small, in particular, much smaller than $\lambda|\vec{f}|$. Making use of Eq. (67), hyper wave-structure function, \mathfrak{D} , and noting that when $\vec{\theta} \equiv 0$ it also provides a definition for the ordinary wave-structure function, \mathcal{D} , we can write Q as

$$\begin{aligned}
 Q(\vec{\theta}, \vec{\rho}, \lambda\vec{f}) &= \frac{8.16}{4\pi^2} k^2 \int_{\text{PATH}} dv C_N^2 \int d\vec{\kappa} \kappa^{-11/3} \\
 &\quad \{ \frac{1}{2} \exp[i\vec{\kappa} \cdot (\vec{\rho} + \lambda\vec{f})] - \exp[i\vec{\kappa} \cdot \vec{\rho}] + \frac{1}{2} \exp[i\vec{\kappa} \cdot (\vec{\rho} - \lambda\vec{f})] \} \\
 &\quad \times \{ -\exp(i\vec{\kappa} \cdot \vec{\theta}v) + 2 - \exp(-i\vec{\kappa} \cdot \vec{\theta}v) \} \\
 &= -\frac{8.16}{8\pi^2} k^2 \int_{\text{PATH}} dv C_N^2 \int d\vec{\kappa} \kappa^{-11/3} \exp(i\vec{\kappa} \cdot \vec{\rho}) \\
 &\quad \times [\exp(i\vec{\kappa} \cdot \lambda\vec{f}/2) - \exp(-i\vec{\kappa} \cdot \lambda\vec{f}/2)]^2 \\
 &\quad \times [\exp(i\vec{\kappa} \cdot \vec{\theta}v/2) - \exp(-i\vec{\kappa} \cdot \vec{\theta}v/2)]^2 \\
 &= \frac{8.16}{2\pi^2} k^2 \int_{\text{PATH}} dv C_N^2 \int d\vec{\kappa} \kappa^{-11/3} \exp(i\vec{\kappa} \cdot \vec{\rho}) \\
 &\quad \times \sin^2(\frac{1}{2} \lambda\vec{f} \cdot \vec{\kappa}) [\exp(i\vec{\kappa} \cdot \vec{\theta}v/2) - \exp(-i\vec{\kappa} \cdot \vec{\theta}v/2)]^2. \quad (75)
 \end{aligned}$$

At this point we note that $\lambda|\vec{f}|$ is very large compared to r_0 and thus large with respect to all of the values of ρ and of θv of interest. As a consequence we may argue that the $\sin^2(\frac{1}{2} \lambda\vec{f} \cdot \vec{\kappa})$ term goes through

many oscillations in any locality of the $\vec{\kappa}$ -space integration, and therefore may be considered to have an approximate value of one-half. Thus we may rewrite Eq. (75) as

$$Q(\vec{\vartheta}, \vec{\rho}, \lambda \vec{f}) = \frac{8 \cdot 16}{4\pi^2} k^2 \int_{\text{PATH}} dv C_N^2 \int d\vec{\kappa} \kappa^{-11/3} \exp(i\vec{\kappa} \cdot \vec{\rho}) \times [\exp(i\vec{\kappa} \cdot \vec{\vartheta} v/2) - \exp(-i\vec{\kappa} \cdot \vec{\vartheta} v/2)]^2. \quad (76)$$

We can rewrite this as

$$Q(\vec{\vartheta}, \vec{\rho}, \lambda \vec{f}) = -\frac{8 \cdot 16}{\pi^2} k^2 \int_{\text{PATH}} dv C_N^2 \int d\vec{\kappa} \kappa^{-11/3} \cos(\vec{\kappa} \cdot \vec{\rho}) \times \sin^2(\vec{\kappa} \cdot \vec{\vartheta} v/2), \quad (77)$$

where we have dropped the imaginary part of $\exp(i\vec{\kappa} \cdot \vec{\rho})$ since it is an odd-function of $\vec{\kappa}$ while all the rest of the integral is an even-function of $\vec{\kappa}$, so that over the infinite range of the $\vec{\kappa}$ -integration its contribution would vanish.

We now further argue that the constraint that we are only interested in small values of $|\vec{\rho}|$, since only small values of $|\vec{r} - \vec{r}'|$ contribute significantly to the value of $\tilde{\mathcal{J}}$, allows us to approximate the isoplanatism constraint by requiring that $\tilde{Q}(\vec{\vartheta})$, where

$$\tilde{Q}(\vec{\vartheta}) = \frac{8 \cdot 16}{\pi^2} k^2 \int_{\text{PATH}} dv C_N^2 \int d\vec{\kappa} \kappa^{-11/3} \sin^2(\vec{\kappa} \cdot \vec{\vartheta} v/2) \quad (78)$$

be less than unity. Here we have replaced $\cos(\vec{\kappa} \cdot \vec{\rho})$ with unity based on the fact that with $|\vec{\rho}|$ small or comparable to r_0 , $\vec{\kappa} \cdot \vec{\rho}$ will not be large for any value of $\vec{\kappa}$ which contributes significantly to the wavefront distortion.

Letting ν denote the angle between $\vec{\kappa}$ and $\vec{\vartheta}$ we can rewrite Eq. (78) as

$$\begin{aligned}\tilde{Q}(\vec{\vartheta}) &= \frac{8.16}{\pi^2} k^2 \int_{\text{PATH}} dv C_N^2 \int_0^\infty d\kappa \kappa^{-2/3} \int_0^{2\pi} d\nu \sin^2 \left[\frac{1}{2} \kappa \vartheta v \cos(\nu) \right] \\ &= \frac{8.16}{2\pi^2} k^2 \int_{\text{PATH}} dv C_N^2 \int_0^\infty d\kappa \kappa^{-2/3} \int_0^{2\pi} d\nu \{1 - \cos[\kappa \vartheta v \cos(\nu)]\} \\ &= \frac{8.16}{\pi} k^2 \int_{\text{PATH}} dv C_N^2 \int_0^\infty d\kappa \kappa^{-2/3} [1 - J_0(\kappa \vartheta v)] .\end{aligned}\quad (79)$$

Making a change of variables, with $x = \kappa \vartheta v$, we can rewrite Eq. (79) as

$$\tilde{Q}(\vec{\vartheta}) = \vartheta^{5/3} \left\{ \frac{8.16}{\pi} k^2 \int_{\text{PATH}} dv v^{5/3} C_N^2 \int_0^\infty dx x^{-2/3} [1 - J_0(x)] \right\} . \quad (80)$$

It is easy to show¹⁴ that

$$\begin{aligned}\int_0^\infty dx x^{-2/3} [1 - J_0(x)] &= -2^{-2/3} \frac{\Gamma(-5/6)}{\Gamma(11/6)} \\ &= 1.1183\end{aligned}\quad (81)$$

so that

$$\tilde{Q}(\vec{\vartheta}) = \vartheta^{5/3} \left\{ 2.91 k^2 \int_{\text{PATH}} dv v^{5/3} C_N^2 \right\} . \quad (82)$$

Thus our criteria for there to be so significant anisoplanatism, that $\tilde{Q}(\vec{\vartheta})$ be less than unity reduces to the condition that

$$\vartheta < \vartheta_0 , \quad (83)$$

where

$$\vartheta_0 = \left\{ 2.91 k^2 \int_{PATH} dv v^{5/3} C_N^2 \right\}^{-3/5} \quad (84)$$

We call ϑ_0 the isoplanatism angle.

In Fig. 6, we show a sample vertical distribution of the optical strength of turbulence, C_N^2 , as reported by Greenwood.¹⁵ Using this distribution, we have calculated the isoplanatism angle for a wavelength $\lambda = 5.5 \times 10^{-7}$ m. We find that in this case $\vartheta_0 = 8.6 \times 10^{-6}$ rad. Our theory predicts that the Labeyrie technique should produce good results when working with a pair of point sources with angular separation less than this, but that if the point sources are separated by an angle greater than this, the high spatial frequency details will be lost, or at least significantly attenuated from what we expect, based on calibration of the technique with a single point source. Referring back to Eq. (73) and noting that \tilde{Q} is the negative of Q , we would expect from consideration of Eq. 's (82) and (84) that the high frequency details will be attenuated approximately as $\exp [-(\vartheta/\vartheta_0)^{5/3}]$ relative to the ability of the Labeyrie technique to accommodate a single point source. From consideration of Eq. (73), we can see that the net effect of a lack of isoplanatism will be to make the source appear more like a single point source. A pair of equal intensity point sources would appear like a pair of unequal intensity point sources, the ratio of intensities appearing to be $\frac{1}{2} \exp [-(\vartheta/\vartheta_0)^{5/3}]$.

With these results in hand, we are now ready to turn our attention to the Knox-Thompson concept. In the next section, we shall describe this concept and then present an analysis of its operation, assuming that we are dealing with a pair of point sources close enough together that there is no anisoplanatism effect. Then in Section 6, we shall extend this analysis to treat the case where the angular separation is large enough for anisoplanatism effects to occur.

5. Knox-Thompson Algorithm: Isoplanatism Assumed

In the absence of anisoplanatism effects and with a "calibration run" against a known point source the Labeyrie technique will produce a useful and valid spatial frequency power spectrum of an object of interest. While this gives us much of the information we need to know about the object, it does not permit formation of the image of the object. We have information on the amplitude of each spatial frequency of the image, but we have no knowledge of the spatial phase shift to be associated with each spatial frequency — so we cannot reconstruct the image.

The basic problem in determining the phase shift stems from the fact that, except for the very lowest spatial frequencies, (namely $|\vec{f}| < r_0/\lambda$), the turbulence induced part of the phase shift introduces an rms spatial phase shift, σ , that is many radians. As a consequence the average of the random spatial frequency component, $S(\vec{f})$, will be so strongly attenuated that we cannot use the ensemble average, $\langle S(\vec{f}) \rangle$, to determine the part of the phase shift due to the image. The attenuation is $\exp(-\sigma^2)$, which is too small to allow any practical use to be obtained from the ensemble average $\langle S(\vec{f}) \rangle$.

In mathematical terms we would write that

$$S(\vec{f}) = A_i A_r \exp [i (\varphi_i + \varphi_r)], \quad (85)$$

where A_i is the image associated amplitude, (which we can determine using the Labeyrie technique), and φ_i is the image associated phase shift which we wish to determine. A_r is the random amplitude factor introduced by turbulence effects and φ_r is the turbulence induced spatial phase shift, whose variance is σ_r^2 . If we determine the (ensemble) average of the random amplitude, $S(\vec{f})$, we get

$$\langle S(\vec{f}) \rangle = \{ \langle A_r \rangle \exp(-\sigma_r^2) \} A_1 \exp(i\varphi_1) . \quad (86)$$

The spatial phase shift information is there and we could easily extract it as the argument of the complex value of $\langle S(\vec{f}) \rangle$, but because of the $\exp(-\sigma^2)$ factor we are dealing with such an unfavorable signal strength situation that we cannot obtain a useful estimate of the spatial phase shift. Our answer will be determined by the noise rather than by the signal.

An alternate approach for the calculation of the image associated spatial phase shift, φ_1 , has been suggested by McGlamery¹⁶. This involves extracting the phase, $(\varphi_1 + \varphi_r)$, from each sample of the random spatial frequency complex amplitude, $S(\vec{f})$, and then (ensemble) averaging this phase shift to obtain $\langle (\varphi_1 + \varphi_r) \rangle$ which, since $\langle \varphi_r \rangle = 0$, should reduce to $\langle (\varphi_1 + \varphi_r) \rangle = \varphi_1$. Unfortunately, due to a combination of noise effects, [irrevocable incorporated into the results by the nonlinearity of the process of calculating the argument of $S(\vec{f})$], and due to a basic 2π -ambiguity, there is an uncertainty of the order of $2\pi N$ in our knowledge of $(\varphi_1 + \varphi_r)$, and as a consequence we do not get a meaningful result when we attempt to determine $\langle (\varphi_1 + \varphi_r) \rangle$.

The calculation of the spatial frequency power spectral density

$$\tilde{S}(\vec{f}) = \langle S^*(\vec{f}) S(\vec{f}) \rangle , \quad (87)$$

does not encounter any difficulty due to the turbulence induced random phase shift, φ_r , since there is a cancellation of this term in taking the product $S^*(\vec{f}) S(\vec{f})$. The Knox-Thompson concept seeks to get around all of the above difficulties by measuring the bispectrum

$$\rho(\vec{f}, \vec{f}') = \langle S^*(\vec{f}') S(\vec{f}) \rangle, \quad (88)$$

where \vec{f} and \vec{f}' are distinct but not very widely different spatial frequencies. As will be seen in this case, the two turbulence induced phase shifts, φ_T and φ_T' , are closely correlated. From this it follows that $\varphi_T - \varphi_T'$, which is the turbulence induced random argument of the complex product $S^*(\vec{f}') S(\vec{f})$, has a small mean square value $\sigma_{\varphi_T}^2$, and so the attenuation factor, $\exp(-\sigma_{\varphi_T}^2)$, encountered in forming the (ensemble) average is of the order of unity. The condition required for this to be the case, i.e., for σ_{φ_T} to be very small, will be seen to be $|\vec{f} - \vec{f}'| < r_0/\lambda$.

We shall start our analysis of the Knox-Thompson concept by considering a pair of point sources with amplitudes A_j and $A_{j'}$, located at angular positions $\vec{\theta}_j$ and $\vec{\theta}_{j'}$. Making use of the intermediate results of Section 3, in particular of Eq. (52), we see that we can write the bispectrum, as defined by Eq. (7), as

$$\begin{aligned} \rho(\vec{f}, \vec{f}') &= \frac{1}{4} |g|^4 \iint d\vec{r} d\vec{r}' W(\vec{r}) W(\vec{r} + \lambda \vec{f}) W(\vec{r}') W(\vec{r}' + \lambda \vec{f}') \\ &\times \langle \{ (A_j)^2 \exp[-2\pi i (\vec{f} - \vec{f}') \cdot \vec{\theta}_j] \exp\{i[\phi(\vec{\theta}_j; \vec{r}) - \phi(\vec{\theta}_j; \vec{r} + \lambda \vec{f}) \\ &\quad + \phi(\vec{\theta}_j; \vec{r}' + \lambda \vec{f}') - \phi(\vec{\theta}_j; \vec{r}')] \} \\ &+ A_j^2 A_{j'}^2 \exp[-2\pi i (\vec{f} \cdot \vec{\theta}_j - \vec{f}' \cdot \vec{\theta}_{j'})] \exp\{\phi(\vec{\theta}_j; \vec{r}) \\ &\quad - \phi(\vec{\theta}_j; \vec{r} + \lambda \vec{f}) + \phi(\vec{\theta}_{j'}; \vec{r}' + \lambda \vec{f}') - \phi(\vec{\theta}_{j'}; \vec{r}') \} \\ &+ A_j^2 A_{j'}^2 \exp[-2\pi i (\vec{f} \cdot \vec{\theta}_{j'} - \vec{f}' \cdot \vec{\theta}_j)] \exp\{i[\phi(\vec{\theta}_{j'}; \vec{r}) \\ &\quad - \phi(\vec{\theta}_{j'}; \vec{r} + \lambda \vec{f}) + \phi(\vec{\theta}_j; \vec{r}' + \lambda \vec{f}') - \phi(\vec{\theta}_j; \vec{r}') \} \\ &+ (A_j)^2 \exp[-2\pi i (\vec{f} - \vec{f}') \cdot \vec{\theta}_{j'}] \exp\{i[\phi(\vec{\theta}_{j'}; \vec{r}) - \phi(\vec{\theta}_{j'}; \vec{r} + \lambda \vec{f}) \\ &\quad - \phi(\vec{\theta}_{j'}; \vec{r}' + \lambda \vec{f}') - \phi(\vec{\theta}_{j'}; \vec{r}')] \} \} \rangle. \quad (89) \end{aligned}$$

Here we have written a product of integrals as a double integral, carried out the multiplication, and grouped terms as appropriate in the integrand.

We now introduce the assumption that the statistics of $\phi(\vec{\theta}_j; \vec{r})$, with respect to $\phi(\vec{\theta}_{j'}; \vec{r}')$ are identical to the statistics of $\phi(\vec{\theta}_j; \vec{r})$ with respect to $\phi(\vec{\theta}_j; \vec{r}')$ — in essence, assuming that $\vec{\theta}_j$ and $\vec{\theta}_{j'}$ are in the same isoplanatic patch. Thus restricting our attention in the balance of this section to the case where isoplanatism is assumed, and making use of Eq. 's (16), (17), and (19), we can rewrite Eq. (89) in the form

$$\begin{aligned}
 \mathcal{J}(\vec{r}, \vec{r}') &= \frac{1}{4} |\mathcal{W}|^4 \iint d\vec{r} d\vec{r}' W(\vec{r}) W(\vec{r} + \lambda \vec{r}) W(\vec{r}') W(\vec{r}' + \lambda \vec{r}') \\
 &\times \exp \left\{ -\frac{1}{2} \{ \mathcal{B}(\lambda \vec{r}) + \mathcal{B}(\lambda \vec{r}') + \mathcal{B}(\vec{r} - \vec{r}') \right. \\
 &\quad \left. + \mathcal{B}(\vec{r} - \vec{r}' + \lambda(\vec{r} - \vec{r}')) - \mathcal{B}(\vec{r} - \vec{r}' + \lambda \vec{r}) - \mathcal{B}(\vec{r} - \vec{r}' - \lambda \vec{r}') \} \right\} \\
 &\times \{ (A_j)^2 \exp [-2\pi i (\vec{r} - \vec{r}') \cdot \vec{\theta}_j] \\
 &\quad + (A_j)^2 (A_{j'})^2 \exp [-2\pi i (\vec{r} \cdot \vec{\theta}_j - \vec{r}' \cdot \vec{\theta}_{j'})] \\
 &\quad + (A_j)^2 (A_{j'})^2 \exp [-2\pi i (\vec{r} \cdot \vec{\theta}_{j'} - \vec{r}' \cdot \vec{\theta}_j)] \\
 &\quad + (A_{j'})^2 \exp [-2\pi i (\vec{r} - \vec{r}') \cdot \vec{\theta}_{j'}] \} .
 \end{aligned} \tag{90}$$

We can rewrite this as

$$\begin{aligned}
 \mathcal{J}(\vec{r}, \vec{r}') &= \frac{1}{4} |\mathcal{W}|^4 \iint d\vec{r} d\vec{r}' W(\vec{r}) W(\vec{r} + \lambda \vec{r}) W(\vec{r}') W(\vec{r}' + \lambda \vec{r}') \\
 &\times \exp \left\{ -\frac{1}{2} \{ \mathcal{B}(\lambda \vec{r}) + \mathcal{B}(\lambda \vec{r}') + \mathcal{B}(\vec{r} - \vec{r}') + \mathcal{B}(\vec{r} - \vec{r}' + \lambda(\vec{r} - \vec{r}')) \right. \\
 &\quad \left. - \mathcal{B}(\vec{r} - \vec{r}' + \lambda \vec{r}) - \mathcal{B}(\vec{r} - \vec{r}' - \lambda \vec{r}') \} \right\} \\
 &\times \{ [(A_j)^2 \exp (-2\pi i \vec{r} \cdot \vec{\theta}_j) + (A_{j'})^2 \exp (-2\pi i \vec{r} \cdot \vec{\theta}_{j'})] \\
 &\quad \times [(A_j)^2 \exp (2\pi i \vec{r}' \cdot \vec{\theta}_j) + (A_{j'})^2 \exp (2\pi i \vec{r}' \cdot \vec{\theta}_{j'})] \} .
 \end{aligned} \tag{91}$$

It is particularly significant to note here that the two square bracket terms in the final curly brackets of Eq. (91) represent the fourier transform of the two point source pattern at spatial frequency \vec{f} (in the first of the square brackets), times the complex conjugate of the fourier transform of the pattern at spatial frequency \vec{f}' (in the second square bracket). As noted previously, the phase shift associated with this product is the difference of the phase of the two spatial frequency components, at \vec{f} and \vec{f}' , of the object pattern — and if we can determine this difference of phase shift for all "adjacent" pairs of spatial frequencies in a matrix covering spatial frequency space, we can determine the absolute phase shift for each spatial frequency component. (The process is essentially equivalent to that described by us elsewhere¹⁷ for determination of wavefront distortion from an array of wavefront tilt measurements.)

The key question is whether or not we can determine the difference of phase shifts from a measurement of the bispectrum, $\mathcal{B}(\vec{f}, \vec{f}')$. This, in turn, is determined by the value of the \vec{f}, \vec{f}' -double integral in Eq. (91). Comparing the integrand here with the corresponding integrand in Eq. (63), for the Labeyrie speckle interferometry technique, we see that the two will be equal when \vec{f} equals \vec{f}' . If \vec{f}' is nearly equal to \vec{f} , then the integrals should have nearly the same value — but exactly what difference between \vec{f} and \vec{f}' is allowable under the expression "nearly equal." We recall that in the series of steps leading up to Eq. (40), and thus also to Eq. (63), it was shown that when \vec{f} and \vec{f}' are exactly equal, the integral had a value of $0.435 (r_0/D)^2 \tau_{0L}(\vec{f})$. In the following, we shall repeat those steps with \vec{f}' nearly but not exactly equal to \vec{f} , and show that if $\lambda |\vec{f} - \vec{f}'| \ll r_0$, then the value of the double integral will be essentially as large as when \vec{f}' is exactly equal to \vec{f} .

It is convenient to start by defining the quantity \mathcal{g} by the expression

$$g = -\frac{1}{2} \{ \mathcal{B}(\lambda \vec{f}) + \mathcal{B}(\lambda \vec{f}') + \mathcal{B}(\vec{f} - \vec{f}') + \mathcal{B}[\vec{f} - \vec{f}' + \lambda(\vec{f} - \vec{f}')] - \mathcal{B}(\vec{f} - \vec{f}' + \lambda \vec{f}) - \mathcal{B}(\vec{f} - \vec{f}' - \lambda \vec{f}') \} \quad (92)$$

Making use of Eq. (22), we can write

$$g = 3.44 r_0^{-5/3} [\lambda f^{5/3} + (\lambda f')^{5/3} + |\vec{f} - \vec{f}'|^{5/3} + |\vec{f} - \vec{f}' + \lambda(\vec{f} - \vec{f}')|^{5/3} - |\vec{f} - \vec{f}' + \lambda \vec{f}|^{5/3} - |\vec{f} - \vec{f}' - \lambda \vec{f}'|^{5/3}] \quad (93)$$

which expression we may usefully compare with Eq. (23). In our previous treatment of the Labeyrie technique, developed from Eq. (23), with Eq. (18) playing the same role as Eq. (21) in defining the range of values of \vec{f} and \vec{f}' to be considered and the weighting to be assigned to each (\vec{f}, \vec{f}') -value, we found that when λf was much greater than r_0 , then because there were some very "convenient" cancellation of terms in the approximation for Eq. (23) when $|\vec{f} - \vec{f}'|$ was much less than λf , it followed that the value of the (\vec{f}, \vec{f}') -integration was determined by the range of integration in which $|\vec{f} - \vec{f}'|$ was less than or about equal to r_0 . In the same way, we may expect here that when there is negligible difference between the values of \vec{f} and \vec{f}' , and $\lambda \vec{f}$ is much larger than r_0 , then the value of the (\vec{f}, \vec{f}') -integration in Eq. (91) will be determined by the contribution from the region in which $|\vec{f} - \vec{f}'|$ is less than or about equal to r_0 . This means that as a practical matter in evaluating the bispectrum, $\mathcal{J}(\vec{f}, \vec{f}')$ for λf much greater than r_0 , and \vec{f} and \vec{f}' nearly equal, we can approximate g from Eq. (93) subject to the assumption that $|\vec{f} - \vec{f}'|$ is less than or about equal to r_0 .

Making use of Eq. (25) and equivalent approximations, we can now rewrite Eq. (93) as

$$g = 3.44 r_0^{-5/3} \left[|\vec{f} - \vec{f}'|^{5/3} + |\vec{f} - \vec{f}' + \lambda(\vec{f} - \vec{f}')|^{5/3} + \frac{5}{3} (\lambda f)^{-1/3} (\vec{f} - \vec{f}') \cdot \lambda(\vec{f} - \vec{f}') + \frac{5}{3} (\lambda f)^{-1/3} (\vec{f} - \vec{f}') \cdot \lambda \vec{f} \frac{\vec{f} \cdot (\vec{f} - \vec{f}')}{f^2} \right] \quad (94)$$

It is immediately apparent from consideration of Eq. (94) substituted into Eq. (91) that the key question in determining the value of the integral is whether $\lambda|\vec{r}-\vec{r}'|$ is greater than r_0 , or less. In either case, the result is not significantly dependent on anything except the $|\vec{r}-\vec{r}'|^{5/3}$ and the $|\vec{r}-\vec{r}'+\lambda(\vec{r}-\vec{r}')|^{5/3}$ terms in Eq. (94). We can rewrite Eq. (91) as

$$\begin{aligned} \mathcal{J}(\vec{f}, \vec{f}') &\approx \frac{1}{4} |y|^4 \iint d\vec{r} d\vec{r}' W(\vec{r}) W(\vec{r}+\lambda\vec{f}) W(\vec{r}') W(\vec{r}'+\lambda\vec{f}') \\ &\times \exp \{ -3.44 r_0^{-5/3} [|\vec{r}-\vec{r}'|^{5/3} + |\vec{r}-\vec{r}'+\lambda(\vec{r}-\vec{r}')|^{5/3}] \} \\ &\times \{ [(A_j^2) \exp (-2\pi i \vec{f} \cdot \vec{\theta}_j) + (A_{j'}^2) \exp (-2\pi i \vec{f}' \cdot \vec{\theta}_{j'})] \\ &\times [(A_j^2) \exp (2\pi i \vec{f}' \cdot \vec{\theta}_j) + (A_{j'}^2) \exp (2\pi i \vec{f} \cdot \vec{\theta}_{j'})] \} \quad (95) \end{aligned}$$

For the required condition for successful operation of the Knox-Thompson technique, i.e., for $\lambda(\vec{r}-\vec{r}')$ much less than r_0 , and recalling that the value of the integral is determined, for the most part, by the region in which $|\vec{r}-\vec{r}'|$ is of the order of r_0 , we see that Eq. (95) reduces to

$$\begin{aligned} \mathcal{J}(\vec{f}, \vec{f}') &\approx \frac{1}{4} |y|^4 \iint d\vec{r} d\vec{r}' W(\vec{r}) W(\vec{r}+\lambda\vec{f}) W(\vec{r}') W(\vec{r}'+\lambda\vec{f}') \\ &\times \exp [-6.88 (|\vec{r}-\vec{r}'|/r_0)^{5/3}] \\ &\times \{ [(A_j^2) \exp (-2\pi i \vec{f} \cdot \vec{\theta}_j) + (A_{j'}^2) \exp (-2\pi i \vec{f}' \cdot \vec{\theta}_{j'})] \\ &\times [(A_j^2) \exp (2\pi i \vec{f}' \cdot \vec{\theta}_j) + (A_{j'}^2) \exp (2\pi i \vec{f} \cdot \vec{\theta}_{j'})] \} \quad (96) \end{aligned}$$

This integral was previously encountered in Eq. (30) and evaluated in Eq. (39). Making use of Eq. (21), we see that with this integral evaluation, we can write the normalized bispectrum as

$$\begin{aligned} \frac{\mathcal{J}(\vec{f}, \vec{f}')}{\mathcal{J}(0, 0)} &= \{ 0.435 (r_0/D)^2 \tau_{bl}(\vec{f}) \} \\ &\times \{ [(A_j^2) \exp (-2\pi i \vec{f} \cdot \vec{\theta}_j) + (A_{j'}^2) \exp (-2\pi i \vec{f}' \cdot \vec{\theta}_{j'})] \\ &\times [(A_j^2) \exp (2\pi i \vec{f}' \cdot \vec{\theta}_j) + (A_{j'}^2) \exp (2\pi i \vec{f} \cdot \vec{\theta}_{j'})] \\ &\times [(A_j^2) + (A_{j'}^2)]^{-2} \} \quad (97) \end{aligned}$$

The leading curly bracket term is the quantity of interest. It represents the ability of the process to "avoid" washing out the information carrying part of the signal because of averaging over a large range of phase fluctuations. The larger the curly bracket term is, the better the system may be considered to perform. We note that with $\lambda|\vec{r}-\vec{r}'|$ smaller than r_0 , the system's ability to avoid signal washout is as good as for the Labeyrie speckle interferometry technique.

If we violate the requirement that $\lambda|\vec{r}-\vec{r}'|$ is to be less than r_0 , then since the value of the double integral in Eq. (95) comes principally from the (\vec{r}, \vec{r}') region of integration where $|\vec{r}-\vec{r}'|$ is less than r_0 , we can approximate Eq. (95) by the expression

$$\begin{aligned} \mathcal{J}(\vec{r}, \vec{r}') &= \exp [-3.44 (\lambda|\vec{r}-\vec{r}'|/r_0)^{5/3}] \frac{1}{4} |\mathcal{U}|^4 \\ &\times \iint d\vec{r} d\vec{r}' \exp [-3.44 (|\vec{r}-\vec{r}'|/r_0)^{5/3}] \\ &\times W(\vec{r}) W(\vec{r}+\lambda\vec{r}) W(\vec{r}') W(\vec{r}'+\lambda\vec{r}') \\ &\times \{ [(A_j^2) \exp (-2\pi i \vec{r} \cdot \vec{\theta}_j) + (A_{j'}^2) \exp (-2\pi i \vec{r}' \cdot \vec{\theta}_{j'})] \\ &\times [(A_j^2) \exp (2\pi i \vec{r}' \cdot \vec{\theta}_j) + (A_{j'}^2) \exp (2\pi i \vec{r} \cdot \vec{\theta}_{j'})] \} . \end{aligned} \quad (98)$$

Except for a slight change of coefficient in the exponent [which we can "get rid of" by replacing $3.44 r_0^{-5/3}$ by $6.88 (1.516 r_0)^{-5/3}$], the integral is the same one which we just evaluated. Carrying out the integration and normalizing as before, in this case we get

$$\begin{aligned} \frac{\mathcal{J}(\vec{r}, \vec{r}')}{\mathcal{J}(0,0)} &= \left\{ \exp \left[-3.44 \left(\frac{\lambda|\vec{r}-\vec{r}'|}{r_0} \right)^{5/3} \right] \left(\frac{r_0}{D} \right) \tau_{bl}(\vec{r}) \right\} \\ &\times \{ [(A_j^2) \exp (-2\pi i \vec{r} \cdot \vec{\theta}_j) + (A_{j'}^2) \exp (-2\pi i \vec{r}' \cdot \vec{\theta}_{j'})] \\ &\times [(A_j^2) \exp (2\pi i \vec{r}' \cdot \vec{\theta}_j) + (A_{j'}^2) \exp (2\pi i \vec{r} \cdot \vec{\theta}_{j'})] \\ &\times [(A_j^2) + (A_{j'}^2)]^{-2} \} . \end{aligned} \quad (99)$$

It is immediately apparent from inspection of this result that if we allow the frequency difference to be large, i.e., if $\lambda|\vec{f}-\vec{f}'|$ is larger than r_0 , the Knox-Thompson technique will produce poor results, i.e., the information carrying part of the signal will be washed out.

From a comparison of Eq. 's (97) and (99), we can form an estimate of how much smaller than r_0 we should require $\lambda|\vec{f}-\vec{f}'|$ to be. We form our estimate based on the requirement that the knee of the curve of $|\vec{f}-\vec{f}'|$ dependence should correspond to the value where the two (asymptotic) dependencies intersect. This occurs where

$$\exp [-3.44 (\lambda|\vec{f}-\vec{f}'|_K/r_0)^{5/3}] = 0.435 \quad , \quad (100)$$

where the subscript K denotes the "knee" value. Solving this equation, we get

$$\lambda|\vec{f}-\vec{f}'|_K = 0.427 r_0 \quad . \quad (101)$$

Based on this result, we would suggest that for proper implementation of the Knox-Thompson algorithm, the data processing should be done with an array of spatial frequencies whose frequency spacing is no greater than $0.4 r_0/\lambda$, and preferably no greater than $0.2 r_0/\lambda$.

With this result in hand, we are now ready to proceed to the analysis of the Knox-Thompson algorithm in the case where the angular separation, $\vec{\theta}_1 - \vec{\theta}_2$, of the two point sources is large enough that there will be anisoplanatism effects. We take this up next, in Section 6.

6. Knox-Thompson Algorithm: Anisoplanatism

We start our analysis of the effect of anisoplanatism on the Knox-Thompson algorithm with Eq. (89). Here, unlike our procedure in the last section, we shall not introduce the assumption that the wavefront distortion, $\phi(\vec{\theta}; \vec{r})$, is independent of the exact value of $\vec{\theta}$. Making use of Eq.'s (16), (17), and (19), we can recast this as

$$\begin{aligned}
 J(\vec{f}, \vec{f}') = & \frac{1}{2} |u|^4 \iint d\vec{r} d\vec{r}' W(\vec{r}) W(\vec{r} + \lambda \vec{f}) W(\vec{r}') W(\vec{r}') W(\vec{r}' + \lambda \vec{f}') \\
 & \times \left\{ (A_j^2)^2 \exp[-2\pi i (\vec{f} - \vec{f}') \cdot \vec{\theta}_j] \exp\left(-\frac{1}{2} \{ \mathcal{D}(\lambda \vec{f}) - \mathcal{D}(\vec{r} - \vec{r}' - \lambda \vec{f}') \right. \right. \\
 & \quad \left. \left. + \mathcal{D}(\vec{r} - \vec{r}') + \mathcal{D}[\vec{r} - \vec{r}' + \lambda(\vec{f} - \vec{f}')] - \mathcal{D}(\vec{r} - \vec{r}' + \lambda \vec{f}) + \mathcal{D}(\lambda \vec{f}') \} \right) \right. \\
 & + A_j^2 A_{j'}^2 \exp[-2\pi i (\vec{f} \cdot \vec{\theta}_j - \vec{f}' \cdot \vec{\theta}_{j'})] \exp\left(-\frac{1}{2} \{ \mathcal{D}(\lambda \vec{f}) - \langle \phi(\vec{\theta}_j; \vec{r}) \right. \right. \\
 & \quad \left. \left. - \phi(\vec{\theta}_{j'}; \vec{r}' + \lambda \vec{f}') \rangle^2 \right) \right. \\
 & + \langle [\phi(\vec{\theta}_j; \vec{r}) - \phi(\vec{\theta}_{j'}; \vec{r}')]^2 \rangle + \langle [\phi(\vec{\theta}_j; \vec{r} + \lambda \vec{f}) - \phi(\vec{\theta}_{j'}; \vec{r}' + \lambda \vec{f}')]^2 \rangle \\
 & \quad \left. - \langle [\phi(\vec{\theta}_j; \vec{r} + \lambda \vec{f}) - \phi(\vec{\theta}_{j'}; \vec{r}')]^2 \rangle + \mathcal{D}(\lambda \vec{f}') \} \right) \\
 & + A_j^2 A_{j'}^2 \exp[-2\pi i (\vec{f} \cdot \vec{\theta}_{j'} - \vec{f}' \cdot \vec{\theta}_j)] \exp\left(-\frac{1}{2} \{ \mathcal{D}(\lambda \vec{f}) - \langle \phi(\vec{\theta}_j; \vec{r}) \right. \right. \\
 & \quad \left. \left. - \phi(\vec{\theta}_j; \vec{r}' + \lambda \vec{f}') \rangle^2 \right) \right. \\
 & + \langle [\phi(\vec{\theta}_j; \vec{r}) - \phi(\vec{\theta}_j; \vec{r}')]^2 \rangle + \langle [\phi(\vec{\theta}_j; \vec{r} + \lambda \vec{f}) - \phi(\vec{\theta}_j; \vec{r}' + \lambda \vec{f}')]^2 \rangle \\
 & \quad \left. - \langle [\phi(\vec{\theta}_j; \vec{r} + \lambda \vec{f}) - \phi(\vec{\theta}_j; \vec{r}')]^2 \rangle + \mathcal{D}(\lambda \vec{f}') \} \right) \\
 & + (A_{j'}^2)^2 \exp[-2\pi i (\vec{f} - \vec{f}') \cdot \vec{\theta}_{j'}] \exp\left(-\frac{1}{2} \{ \mathcal{D}(\lambda \vec{f}) - \mathcal{D}(\vec{r} - \vec{r}' - \lambda \vec{f}') \right. \right. \\
 & \quad \left. \left. + \mathcal{D}(\vec{r} - \vec{r}') + \mathcal{D}[\vec{r} - \vec{r}' + \lambda(\vec{f} - \vec{f}')] - \mathcal{D}(\vec{r} - \vec{r}' + \lambda \vec{f}) + \mathcal{D}(\lambda \vec{f}') \} \right) \right\} . \quad (102)
 \end{aligned}$$

We now make use of the symmetrization argument used to let us go from Eq. (58) to Eq. (60). We then note that we can now repeat essentially the same manipulations we used in Eq. (68) and Eq. (69). The equivalence of

these equations allows us to rewrite our results in terms of the hyper wave-structure function, as defined by Eq. (66), so that we obtain in place of Eq. (102) the result that

$$\begin{aligned}
 \mathcal{J}(\vec{f}, \vec{f}') &= \frac{1}{4} |u|^4 \iint d\vec{r} d\vec{r}' W(\vec{r}) W(\vec{r}+\lambda\vec{f}) W(\vec{r}') W(\vec{r}'+\lambda\vec{f}') \\
 &\times \left\{ [(A_j^a)^2 \exp[-2\pi i (\vec{f}-\vec{f}') \cdot \vec{\theta}_j] + (A_{j'}^a)^2 \exp[-2\pi i (\vec{f}-\vec{f}') \cdot \vec{\theta}_{j'}]] \right. \\
 &\times \exp \left(-\frac{1}{2} \{ \mathcal{D}(\lambda\vec{f}) + \mathcal{D}(\lambda\vec{f}') + \mathcal{D}(\vec{r}-\vec{r}') + \mathcal{D}[\vec{r}-\vec{r}'+\lambda(\vec{f}-\vec{f}')] \right. \\
 &\quad \left. \left. - \mathcal{D}(\vec{r}-\vec{r}'+\lambda\vec{f}) - \mathcal{D}(\vec{r}-\vec{r}'-\lambda\vec{f}') \} \right) \right. \\
 &+ (A_j^a)(A_{j'}^a) \{ \exp[-2\pi i (\vec{f} \cdot \vec{\theta}_j - \vec{f}' \cdot \vec{\theta}_{j'})] + \exp[-2\pi i (\vec{f} \cdot \vec{\theta}_{j'} - \vec{f}' \cdot \vec{\theta}_j)] \} \\
 &\times \exp \left(-\frac{1}{2} \{ \mathcal{D}(\lambda\vec{f}) + \mathcal{D}(\lambda\vec{f}') + \mathcal{D}(\vec{\theta}_j - \vec{\theta}_{j'}; \vec{r}-\vec{r}') + \mathcal{D}[\vec{\theta}_j - \vec{\theta}_{j'}; \vec{r}-\vec{r}'+\lambda(\vec{f}-\vec{f}')] \right. \\
 &\quad \left. \left. - \mathcal{D}(\vec{\theta}_j - \vec{\theta}_{j'}; \vec{r}-\vec{r}'+\lambda\vec{f}) - \mathcal{D}(\vec{\theta}_j - \vec{\theta}_{j'}; \vec{r}-\vec{r}'-\lambda\vec{f}') \} \right) \right\} \quad (103)
 \end{aligned}$$

It is useful to rewrite this equation as

$$\begin{aligned}
 \mathcal{J}(\vec{f}, \vec{f}') &= \frac{1}{4} |u|^4 \iint d\vec{r} d\vec{r}' W(\vec{r}) W(\vec{r}+\lambda\vec{f}) W(\vec{r}') W(\vec{r}'+\lambda\vec{f}') \\
 &\times \exp \left(-\frac{1}{2} \{ \mathcal{D}(\lambda\vec{f}) + \mathcal{D}(\lambda\vec{f}') + \mathcal{D}(\vec{r}-\vec{r}') + \mathcal{D}[\vec{r}-\vec{r}'+\lambda(\vec{f}-\vec{f}')] \right. \\
 &\quad \left. \left. - \mathcal{D}(\vec{r}-\vec{r}'+\lambda\vec{f}) - \mathcal{D}(\vec{r}-\vec{r}'-\lambda\vec{f}') \} \right) \right. \\
 &\times \left((A_j^a)^2 \exp[-2\pi i (\vec{f}-\vec{f}') \cdot \vec{\theta}_j - \vec{\theta}_{j'}] + (A_{j'}^a)^2 \exp[-2\pi i (\vec{f}-\vec{f}') \cdot \vec{\theta}_{j'}] \right. \\
 &+ (A_j^a)(A_{j'}^a) \{ \exp[-2\pi i (\vec{f} \cdot \vec{\theta}_j - \vec{f}' \cdot \vec{\theta}_{j'})] + \exp[-2\pi i (\vec{f} \cdot \vec{\theta}_{j'} - \vec{f}' \cdot \vec{\theta}_j)] \} \\
 &\times \exp \left[\frac{1}{2} \mathcal{D}(\vec{\theta}_j - \vec{\theta}_{j'}; \vec{r}-\vec{r}', \lambda\vec{f}, \lambda\vec{f}') \right] \Big) \quad (104)
 \end{aligned}$$

where

$$\begin{aligned}
 \mathcal{D}(\vec{\theta}_j - \vec{\theta}_{j'}; \vec{r}-\vec{r}', \lambda\vec{f}, \lambda\vec{f}') &= \left([\mathcal{D}(\vec{r}-\vec{r}') - \mathcal{D}(\vec{\theta}_j - \vec{\theta}_{j'}; \vec{r}-\vec{r}')] \right. \\
 &+ \{ \mathcal{D}[\vec{r}-\vec{r}'+\lambda(\vec{f}-\vec{f}')] - \mathcal{D}[\vec{\theta}_j - \vec{\theta}_{j'}; \vec{r}-\vec{r}'+\lambda(\vec{f}-\vec{f}')] \} \\
 &- [\mathcal{D}(\vec{r}-\vec{r}'+\lambda\vec{f}) - \mathcal{D}(\vec{\theta}_j - \vec{\theta}_{j'}; \vec{r}-\vec{r}'+\lambda\vec{f})] \\
 &\left. - [\mathcal{D}(\vec{r}-\vec{r}'-\lambda\vec{f}') - \mathcal{D}(\vec{\theta}_j - \vec{\theta}_{j'}; \vec{r}-\vec{r}'-\lambda\vec{f}')] \right) \quad (105)
 \end{aligned}$$

A comparison of Eq. (104) with Eq. (90) makes it clear that the condition on $|\vec{\theta}_j - \vec{\theta}_j'|$ required in order for there to be no significant anisoplanatism effect is that Ω must have a value close to zero in the relevant region of the (\vec{r}, \vec{r}') integral.

To establish the allowable range of values of $|\vec{\theta}_j - \vec{\theta}_j'|$ for isoplanatism to apply, we shall carry out an evaluation of $\Omega(\vec{\theta}, \vec{\rho}, \lambda \vec{r}, \lambda \vec{r}')$ subject to the conditions that ρ is less than or of the order of r_0 , that λr and $\lambda r'$ are both much greater than r_0 , and that $\lambda |\vec{r} - \vec{r}'|$ is less than r_0 — as these are the conditions we developed in the last section as defining the range in \vec{r}, \vec{r}' and (\vec{r}, \vec{r}') -integration space within which we get significant contributions to the bispectrum, $\mathcal{B}(\vec{r}, \vec{r}')$.

Making use of Eq. (67), we can write

$$\begin{aligned} \Omega(\vec{\theta}, \vec{\rho}, \lambda \vec{r}, \lambda \vec{r}') &= \frac{8.16}{4\pi^2} k^3 \int_{\text{PATH}} dv C_N^2 \int d\vec{\kappa} \kappa^{-11/3} \\ &\times \left(\exp [i\vec{\kappa} \cdot (\vec{\rho} + \lambda \vec{r})] + \exp [i\vec{\kappa} \cdot (\vec{\rho} - \lambda \vec{r}')] \right. \\ &\quad \left. - \exp (i\vec{\kappa} \cdot \vec{\rho}) - \exp \{i\vec{\kappa} \cdot [\vec{\rho} + \lambda (\vec{r} - \vec{r}')] \} \right) \\ &\times \{-\exp (i\vec{\kappa} \cdot \vec{\theta} v) + 2 - \exp (-i\vec{\kappa} \cdot \vec{\theta} v)\} \end{aligned} \quad (106)$$

With a bit of trigonometric manipulation, this can be rewritten as

$$\begin{aligned} \Omega(\vec{\theta}, \vec{\rho}, \lambda \vec{r}, \lambda \vec{r}') &= -\frac{8.16}{\pi^2} k^3 \int_{\text{PATH}} dv C_N^2 \int d\vec{\kappa} \kappa^{-11/3} \\ &\times \exp \{i\vec{\kappa} \cdot [\vec{\rho} + \frac{1}{2} \lambda (\vec{r} - \vec{r}')] \} \\ &\times \{ \sin^2 [\frac{1}{4} \vec{\kappa} \cdot \lambda (\vec{r} - \vec{r}')] - \sin^2 [\frac{1}{4} \vec{\kappa} \cdot \lambda (\vec{r} + \vec{r}')] \} \\ &\times [\exp (i\vec{\kappa} \cdot \vec{\theta} v/2) - \exp (-i\vec{\kappa} \cdot \vec{\theta} v/2)]^2 \end{aligned} \quad (107)$$

We may now proceed almost exactly as we did following Eq. (75).

We start by noting that for virtually all of the $\vec{\kappa}$ -values that contribute significantly to the wavefront distortion process, $\frac{1}{2} \lambda (\vec{f} + \vec{f}')$ is so large that the $\sin^2 [\frac{1}{2} \vec{\kappa} \cdot \lambda (\vec{f} + \vec{f}')]$ term will oscillate rapidly and therefore will have an average value of one-half. Thus we can replace that sinc-function squared by one-half. Also, we note that since all of the rest of the integrand is manifestly symmetric in $\vec{\kappa}$, we can replace $\exp \{i \vec{\kappa} \cdot [\vec{\rho} + \frac{1}{2} \lambda (\vec{f} + \vec{f}')] \}$ by the corresponding cosine-function. Thus we can write in place of Eq. (107)

$$\begin{aligned} \Omega(\vartheta, \vec{\rho}, \lambda \vec{f}, \lambda \vec{f}') = & \frac{16.32}{\pi^2} k^2 \int_{\text{PATH}} dv C_N^2 \int d\vec{\kappa} \kappa^{-11/3} \\ & \times \cos \{ \vec{\kappa} \cdot [\vec{\rho} + \frac{1}{2} \lambda (\vec{f} + \vec{f}')] \} \{ 1 - 2 \sin^2 [\frac{1}{2} \vec{\kappa} \cdot \lambda (\vec{f} + \vec{f}')] \} \\ & \times \sin^2 (\vec{\kappa} \cdot \vec{\rho} v/2) \quad . \end{aligned} \quad (108)$$

From our previous work, we know that we are only interested in values of $|\vec{f} - \vec{f}'|$, and thus of $\vec{\rho}$ which are less than or equal to r_0 . Similarly, we know that we must restrict our attention to the case where $\lambda |\vec{f} - \vec{f}'|$ is less than r_0 . On the other hand, we know that only values of κ which are smaller than r_0^{-1} contribute significantly to the wavefront distortion. It thus follows that to the level of a first approximation, we may treat the cosine-term and the one-minus-two-times-sine-squared-term in the integrand of Eq. (108) as though they had values about equal to unity.

Taking note of these approximations [and recalling the factor of one-half in the final exponent of Eq. (104)], we see that the condition on ϑ for there to be no significant anisoplanatism effect is that the function $\tilde{\Omega}(\vartheta)$, where

$$\tilde{\Omega}(\vartheta) = \frac{16.32}{\pi^2} k^2 \int_{\text{PATH}} dv C_N^2 \int d\vec{\kappa} \kappa^{-11/3} \sin^2 (\vec{\kappa} \cdot \vec{\rho} v/2) \quad , \quad (109)$$

should have a value less than two. Making reference to Eq. (78) and the

discussion there, we see that we have arrived at exactly the same condition on δ , or $|\vec{\theta}_j - \vec{\theta}_j|$, for isoplanatism to apply for the Knox-Thompson algorithm as we previously developed for isoplanatism to apply to the Labeyrie technique. We require that Eq. (83) with Eq. (84) be satisfied for the Knox-Thompson algorithm to yield isoplanatic performance.

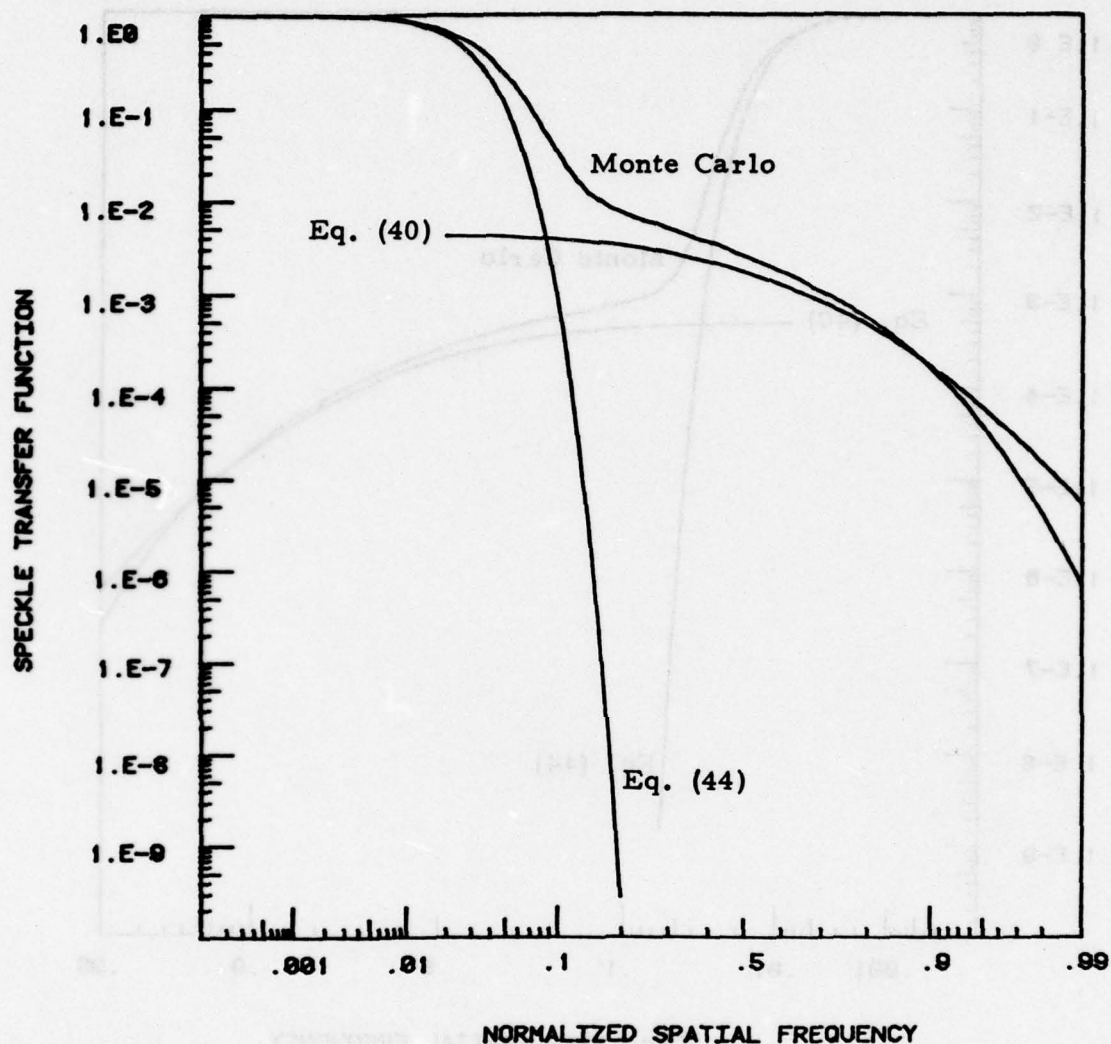


Figure 1. Speckle Transfer Function for $D/r_0 = 10$.

The rapidly decreasing curve represents the low frequency approximation of Eq. (44). The everywhere relatively low level curve represents the high frequency approximation of Eq. (40). The curve running the full range of spatial frequencies represents the Monte Carlo results. The composite of the two approximations can be seen to constitute a fair approximation to the full range result obtained by Monte Carlo methods.

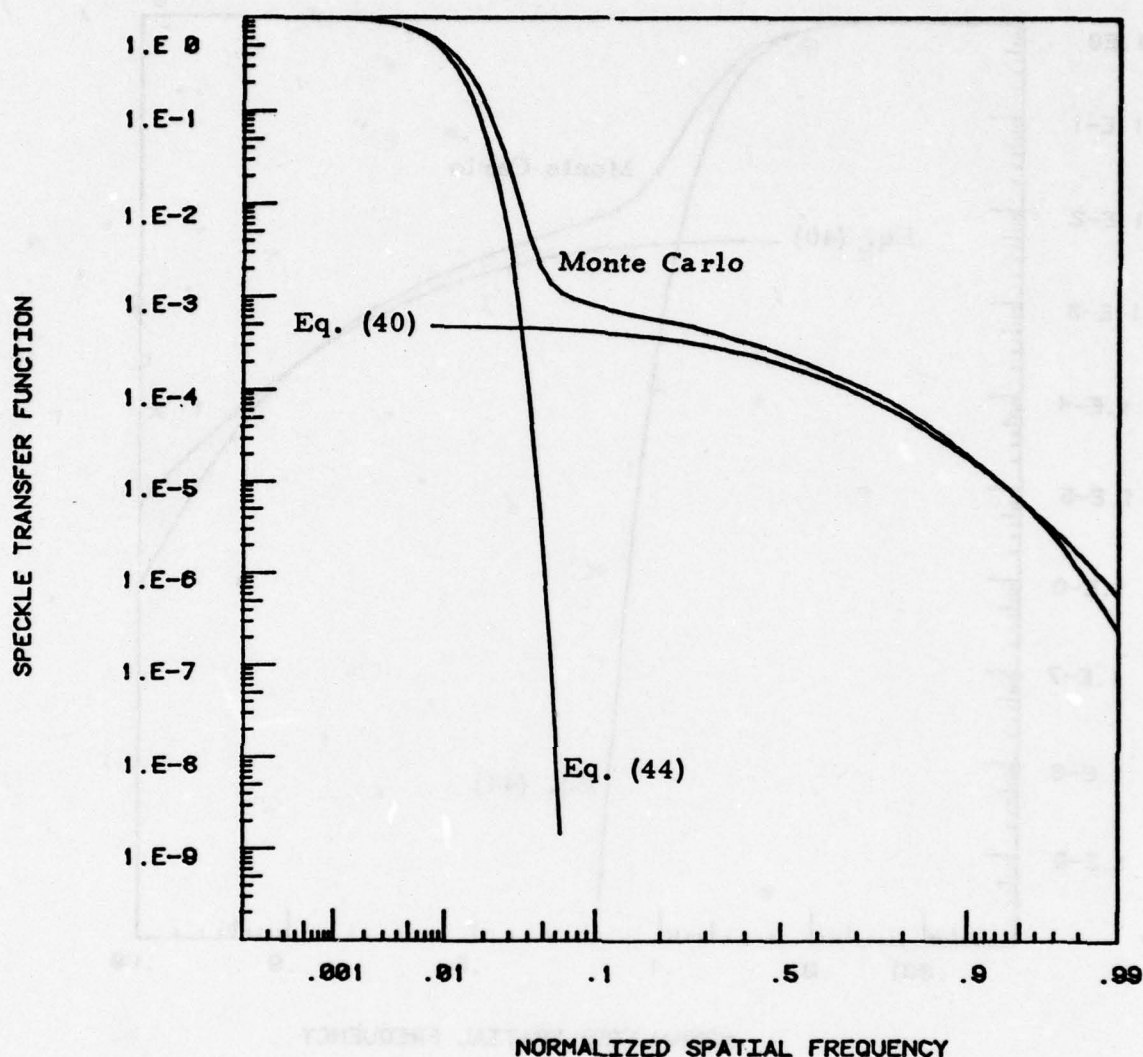


Figure 2. Speckle Transfer Function for $D/r_0 = 30$.

The rapidly decreasing curve represents the low frequency approximation of Eq. (44). The everywhere relatively low level curve represents the high frequency approximation of Eq. (40). The curve running the full range of spatial frequencies represents the Monte Carlo results. The composite of the two approximations can be seen to constitute a fair approximation to the full range result obtained by Monte Carlo methods.

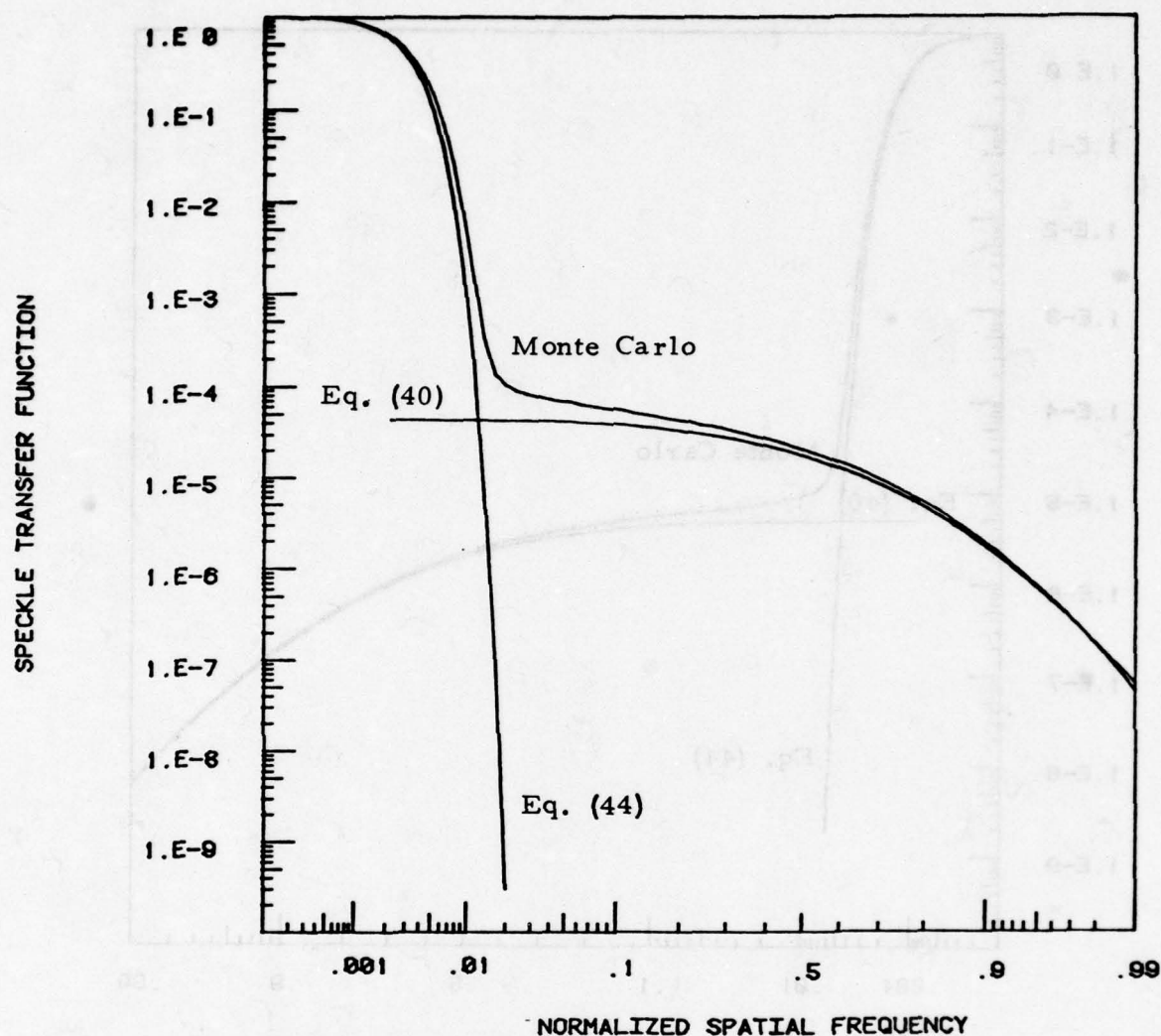


Figure 3. Speckle Transfer Function for $D/r_0 = 100$.

The rapidly decreasing curve represents the low frequency approximation of Eq. (44). The everywhere relatively low level curve represents the high frequency approximation of Eq. (40). The curve running the full range of spatial frequencies represents the Monte Carlo results. The composite of the two approximations can be seen to constitute a fair approximation to the full range result obtained by Monte Carlo methods.

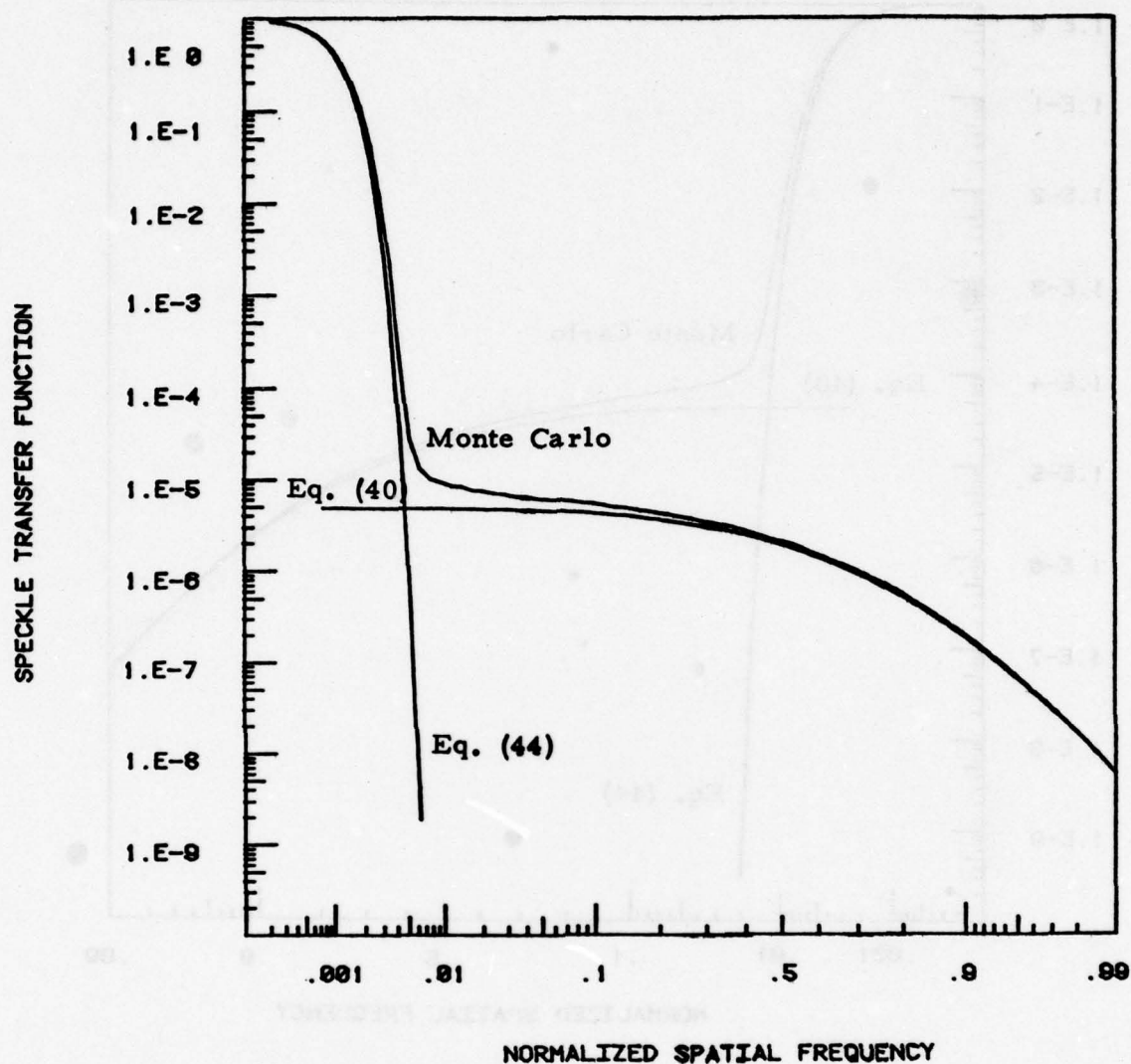


Figure 4. Speckle Transfer Function for $D/r_0 = 300$.

The rapidly decreasing curve represents the low frequency approximation of Eq. (44). The everywhere relatively low level curve represents the high frequency approximation of Eq. (40). The curve running the full range of spatial frequencies represents the Monte Carlo results. The composite of the two approximations can be seen to constitute a fair approximation to the full range result obtained by Monte Carlo methods.

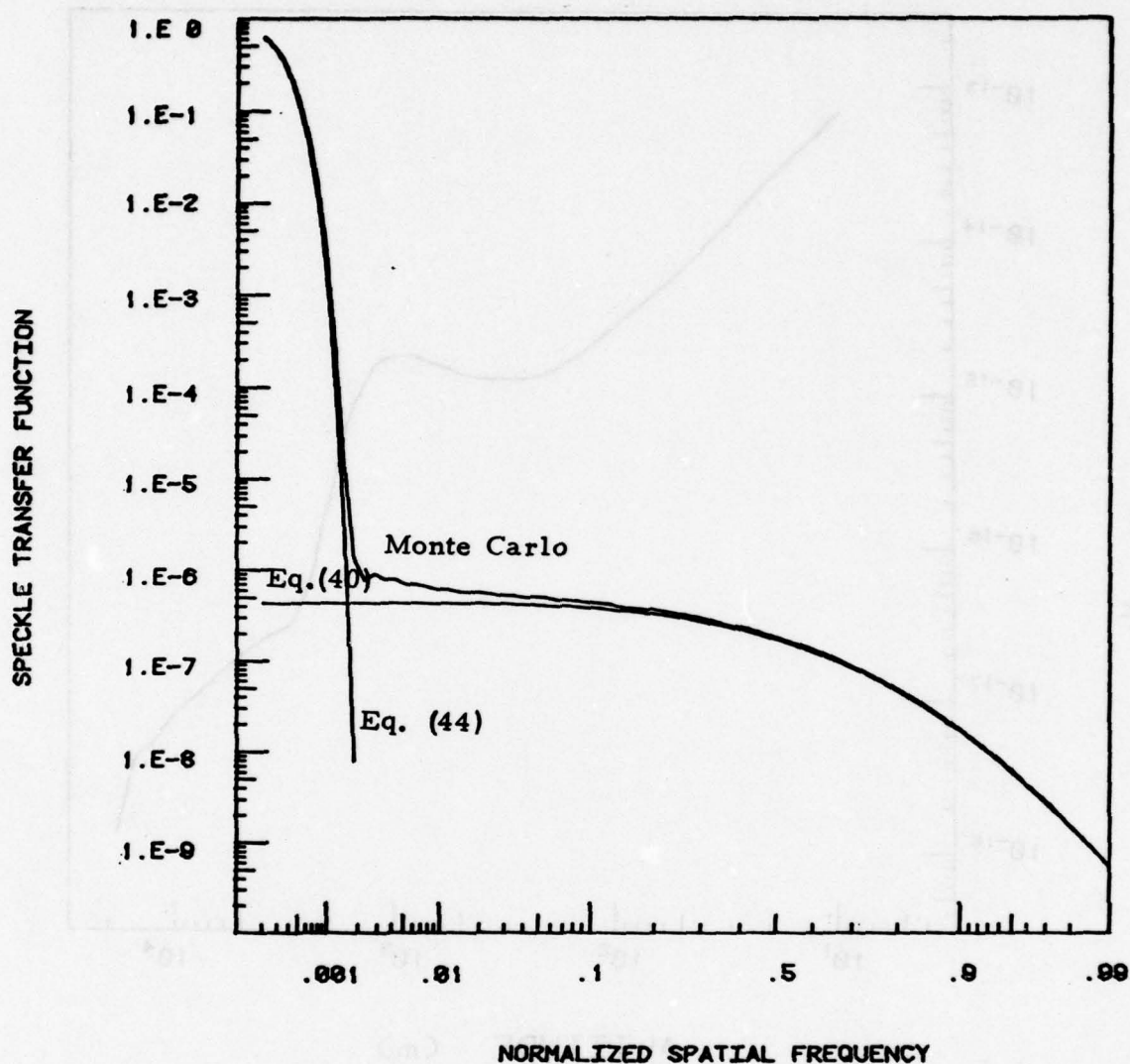


Figure 5. Speckle Transfer Function for $D/r_0 = 1000$.

The rapidly decreasing curve represents the low frequency approximation of Eq. (44). The everywhere relatively low level curve represents the high frequency approximation of Eq. (40). The curve running the full range of spatial frequencies represents the Monte Carlo results. The composite of the two approximations can be seen to constitute a fair approximation to the full range result obtained by Monte Carlo methods.

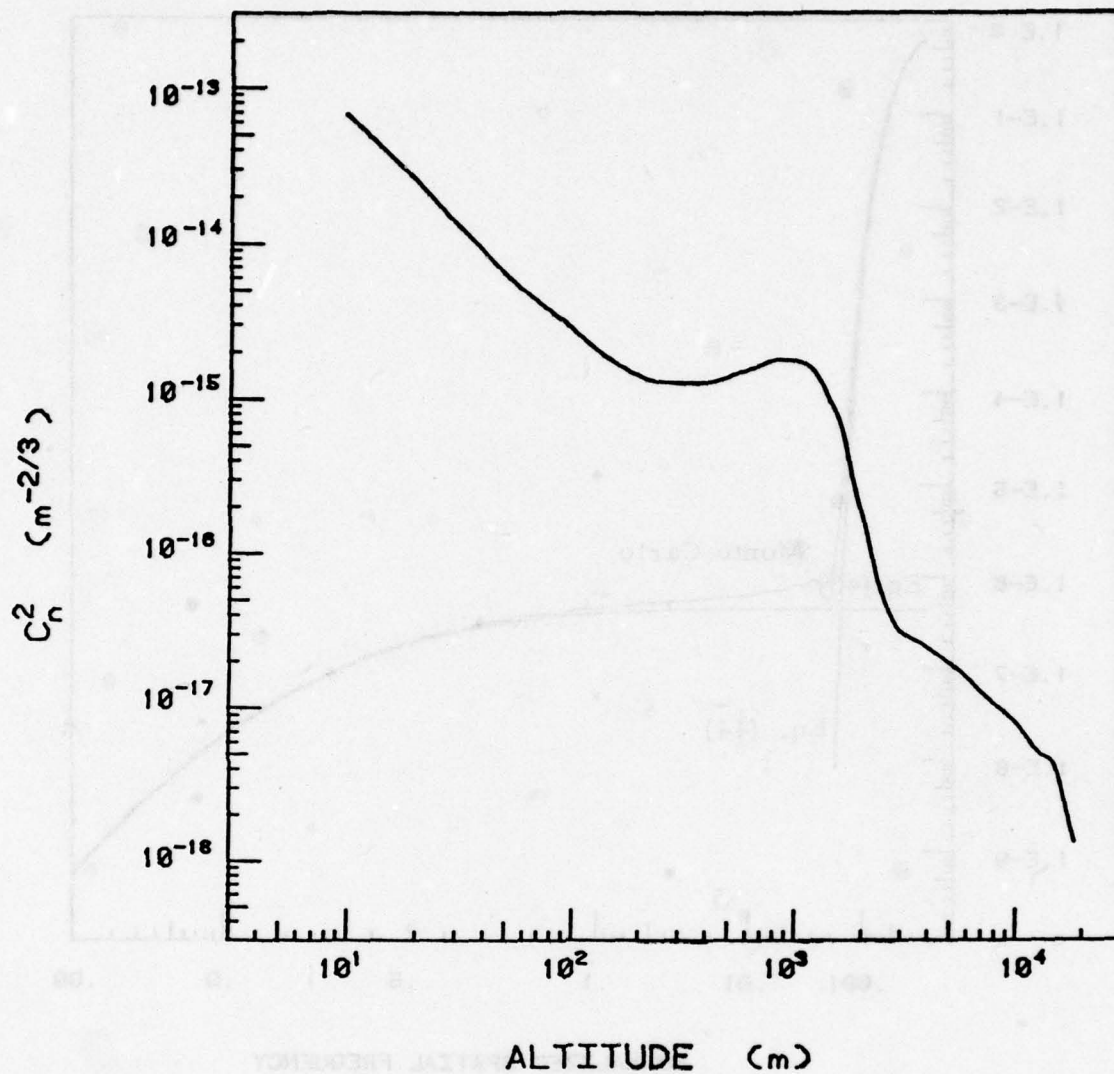


Figure 6. Vertical Distribution of the Refractive-Index Structure Constant.

(From data assembled by D. Greenwood.¹⁵)

References

1. A. Labeyrie, Astr. and Ap. 6, 85 (1970)
2. K. T. Knox and B. J. Thompson, "Recovery of Images From Atmospherically Degraded Short-Exposure Photographs," Ap. J. 193, L45 (1974).
3. D. G. Currie, S. L. Knapp, and K. M. Liewer, Ap. J. 187, 131 (1974). Also, D. G. Currie, "Amplitude Interferometry and High Resolution Image Information," 1974 in: Optical Propagation Through Turbulence, OSA Meeting Digest of Technical Papers, July 1974, Boulder.
4. D. L. Fried, "Varieties of Isoplanatism," Proc. of SPIE 75, 20 (1976).
5. D. L. Fried, "Angle-of-Arrival Isoplanatism," Part II of Theoretical Study of Non-Standard Imaging Concepts, Rome Air Development Center Report No. RADC-TR-76-51, March 1976; and "Isoplanatic Aspects of Predetection Compensation Imagery," Chapter I of Theoretical Study of Non-Standard Imaging Concepts, Rome Air Development Center Report No. RADC-TR-74-185, May 1974.
6. D. Korff, "Analysis of a Method for Obtaining Near-Diffraction-Limited Information in the Presence of Atmospheric Turbulence," J. Opt. Soc. Am. 63, 971 (1973).
7. K. T. Knox, "Diffraction-Limited Imaging With Astronomical Telescopes," in Digest of Papers of the International Optical Computing Conference, April 1975, Washington; sponsored by the Computer Society of the IEEE.
8. V. I. Tatarski, Wave Propagation in a Turbulent Medium (McGraw-Hill Book Co., Inc., New York, 1961).
9. D. L. Fried, "Optical Heterodyne Detection of an Atmospherically Distorted Signal Wave Front," Proc. IEEE 55, 57 (1967).
10. D. L. Fried, "Atmospheric Modulation Noise in an Optical Heterodyne Receiver," IEEE JQE 3, 213 (1967).
11. Op cit Ref. 9; Eq. 's (6.12) and (6.13).
12. Op cit Ref. 8; Eq. (8.20).
13. D. L. Fried, "Spectral and Angular Covariance of Scintillation for Propagation in a Randomly Inhomogeneous Medium," Appl. Opt. 10, 721 (1971).
14. Ibid, Eq. (81)

References (Continued)

15. D. P. Greenwood, private communications.
16. B. L. McGlamery, private communications.
17. D. L. Fried, "Least-Square Fitting A Wave-Front Distortion Estimate To An Array Of Phase-Difference Measurements," J. Opt. Soc. Am. 67, 370 (1977).

Appendix A

Monte Carlo Integral Evaluation

In order to develop a set of values for the frequency dependent speckle image power spectrum, $\tilde{J}(\vec{f})$, in accordance with the exact definition provided by Eq. (18), without introducing any approximations relating to the value of $|\vec{r}-\vec{r}'|/r_0$, or to the value of $\lambda|\vec{f}|/r_0$, in this appendix we shall carry out a numerical evaluation of the integral in Eq. (18) for various values of D/r_0 and of $\lambda|\vec{f}|/r_0$ using Monte Carlo methods. This allows us to test the accuracy of the results we developed in Section 2 of this report using approximations concerning the values of $|\vec{r}-\vec{r}'|/r_0$ and of $\lambda|\vec{f}|/r_0$. The numerical results we shall develop here will show that these approximations lead to quite accurate results.

Making use of Eq. 's (18), (21), and (22), we may write the normalized spectrum, which represents the speckle transfer function, as

$$\begin{aligned} \frac{\tilde{J}(\vec{f})}{\tilde{J}(0)} = & \frac{16}{\pi^2} D^{-4} \iint d\vec{r} d\vec{r}' W(\vec{r}) W(\vec{r}+\lambda\vec{f}) W(\vec{r}') W(\vec{r}'+\lambda\vec{f}) \\ & \times \exp \left\{ -6.88 r_0^{-5/3} \left[|\vec{r}-\vec{r}'|^{5/3} + |\lambda\vec{f}|^{5/3} \right. \right. \\ & \left. \left. - \frac{1}{2} (|\vec{r}-\vec{r}'+\lambda\vec{f}|^{5/3} + |\vec{r}-\vec{r}'-\lambda\vec{f}|^{5/3}) \right] \right\} \end{aligned} \quad (A.1)$$

It will prove convenient for us to make a change of the variables of integration here. For this purpose, we define the variables \vec{x} and \vec{p} according to the equations

$$\vec{x} = \vec{r}/D, \quad (A.2)$$

from which it follows that

$$d\vec{x} = d\vec{r}/D^2, \quad (A.2')$$

and

$$\vec{p} = (\vec{r} - \vec{r}')/D, \quad (A.3)$$

from which (treating \vec{r} as a constant) it follows that

$$d\vec{p} = d\vec{r}'/D^2. \quad (A.3')$$

We can now rewrite the speckle transfer function of Eq. (A.1) as

$$\begin{aligned} \frac{J(\vec{r})}{J(0)} &= \left(\frac{1}{2}\pi\right)^{-2} \iint d\vec{x} d\vec{p} \chi(\vec{x}) \chi(\vec{x} + \vec{a}) \chi(\vec{x} - \vec{p}) \chi(\vec{x} - \vec{p} + \vec{a}) \\ &\times \exp \left\{ -6.88 (D/r_0)^{5/3} \left[|\vec{p}|^{5/3} + |\vec{a}|^{5/3} \right. \right. \\ &\quad \left. \left. - \frac{1}{2} (|\vec{p} + \vec{a}|^{5/3} + |\vec{p} - \vec{a}|^{5/3}) \right] \right\}, \end{aligned} \quad (A.4)$$

where

$$\chi(\vec{x}) = \begin{cases} 1, & \text{if } |\vec{x}| \leq \frac{1}{2} \\ 0, & \text{if } |\vec{x}| > \frac{1}{2} \end{cases}, \quad (A.5)$$

and

$$\vec{a} = \lambda \vec{r}/D, \quad (A.6)$$

represents the normalized spatial frequency. (The effective range of the normalized spatial frequency is from zero to unity.)

It is convenient to rewrite Eq. (A.4) as

$$\begin{aligned} \frac{J(\vec{r})}{J(0)} &= \left(\frac{1}{2}\pi\right)^{-2} \iint d\vec{x} d\vec{p} \chi(\vec{x}) \chi(\vec{x} + \vec{a}) \chi(\vec{x} - \vec{p}) \chi(\vec{x} - \vec{p} + \vec{a}) \\ &\times \exp \left[-6.88 (D/r_0)^{5/3} \psi(\vec{p}, \vec{a}) \right], \end{aligned} \quad (A.7)$$

where

$$\Psi(\vec{p}, \vec{\alpha}) = |\vec{p}|^{5/3} + |\vec{\alpha}|^{5/3} - \frac{1}{2} (|\vec{p} + \vec{\alpha}|^{5/3} + |\vec{p} - \vec{\alpha}|^{5/3}) \quad . \quad (\text{A. 8})$$

Making use of Eq. (24), we note that accordingly as $|\vec{\alpha}|$ is much greater than or much smaller than $|\vec{p}|$, we can approximate $\Psi(\vec{p}, \vec{\alpha})$ by the expressions

$$\Psi(\vec{p}, \vec{\alpha}) \approx |\vec{\alpha}|^{5/3} - \frac{5}{6} |\vec{\alpha}|^2 |\vec{p}|^{-1/3} \left(1 - \frac{1}{3} \frac{(\vec{\alpha} \cdot \vec{p})^2}{|\vec{\alpha}|^2 |\vec{p}|^2} \right) \quad \text{if } |\vec{\alpha}| \ll |\vec{p}| \quad , \quad (\text{A. 9})$$

and

$$\Psi(\vec{p}, \vec{\alpha}) \approx |\vec{p}|^{5/3} - \frac{5}{6} |\vec{p}|^2 |\vec{\alpha}|^{-1/3} \left(1 - \frac{1}{3} \frac{(\vec{\alpha} \cdot \vec{p})^2}{|\vec{\alpha}|^2 |\vec{p}|^2} \right) \quad \text{if } |\vec{\alpha}| \gg |\vec{p}| \quad . \quad (\text{A. 10})$$

We shall not use these approximations in an analytic way to develop our results (as was done in Section 2 of this report), but rather will use Eq. 's (A. 9) and (A. 10) to provide guidance in the selection of the sampling function we shall use for the Monte Carlo evaluation. We shall also use these equations in our numerical computations to assure adequate accuracy in the evaluation of $\Psi(\vec{p}, \vec{\alpha})$ when the magnitudes of $|\vec{p}|$ and $|\vec{\alpha}|$ are greatly different, without resorting to double precision computer computation.

For Monte Carlo evaluation of the integral in Eq. (A. 7), we shall try to use sampling distributions for \vec{x} and \vec{p} that will fully sample the range of allowed values of \vec{x} and \vec{p} , but in such a way as to minimize the "variability of the integrand." This minimization of the variability of the integrand is achieved by making use of the fact that for Monte Carlo

integral evaluation, we can multiply and divide the integrand by any desired probability density and then "extract" the probability density function in the numerator for use as the random sampling density generator. The original integrand divided by the probability density is left as a modified integrand, whose mean value over the sampling density we wish to determine. This mean value, which we estimate as a Monte Carlo average, represents the value of the integral. The accuracy with which the Monte Carlo procedure will estimate the mean value of this modified integrand depends on the variability of the integrand in the sampling range. If we have been reasonably clever in our choice of the sampling distribution, the modified integrand will have a limited variability and it will take relatively few samples to achieve the desired accuracy. If we have not been so clever, more samples will be required. Either way, the validity of the result is unaffected — it is just a matter of how many samples we need to use to achieve the desired accuracy with our Monte Carlo integral evaluation procedure.* In general, and for the problem we are treating here, it is not clear what practical sampling distribution is optimum, and the matter of making an efficient choice is somewhat of an art. We can judge our success in making a suitable choice of the sampling probability density by evaluating not only the mean value but also the standard deviation of the modified integrand when we generate our Monte Carlo average, and in fact we can use this standard deviation to help us decide when we have taken enough random samples.

For Monte Carlo evaluation of the integral in Eq. (A. 7), we chose to use a uniform distribution for \vec{x} and a gaussian distribution for \vec{p} . We chose the range of the \vec{x} -distribution to correspond to the rectangle that just encloses the region of overlap of the two circles defined by $\mathcal{N}(\vec{x})$ and $\mathcal{N}(\vec{x} + \vec{a})$. (Outside this rectangle, the integrand has zero value

* It will later become clear from a study of Table A. 2 that we have not been very clever in our choice of the sampling distribution when D/r_0 is very large and $|\vec{a}| \approx r_0/D$.

so nothing is excluded by use of the limited sampling range.) If we denote the component of \vec{x} that is parallel to $\vec{\alpha}$ by x_1 , and the perpendicular component by x_2 , then our rectangle corresponds to the region defined by the equations

$$-\frac{1}{2} < x_1 < \frac{1}{2} - |\vec{\alpha}| \quad , \quad (A.11a)$$

$$-\frac{1}{2} h x_2 < \frac{1}{2} h \quad , \quad (A.11b)$$

where

$$h = (1 - |\vec{\alpha}|^2)^{1/2} \quad (A.12)$$

This is a rectangle of width $(1 - |\vec{\alpha}|)$ and of height (h) . The probability density function is thus

$$P_u(\vec{x}) = \begin{cases} [(1 - |\vec{\alpha}|) h]^{-1}, & \text{if } \{-\frac{1}{2} < x_1 < \frac{1}{2} - |\vec{\alpha}| \} \\ & \text{and } \{-\frac{1}{2} h < x_2 < \frac{1}{2} h \} \\ 0 & , \text{ otherwise} \end{cases} \quad (A.13)$$

As remarked above, we will use a (two-dimensional) gaussian probability density for the \vec{p} sampling distribution. We can write this as

$$P_g(\vec{p}) = (2\pi\sigma^2)^{-1} \exp(-\frac{1}{2} |\vec{p}|^2 / \sigma^2) \quad , \quad (A.14)$$

where σ is a sampling parameter whose value we have to choose. To get some insight into how to choose a value for σ , we multiply and divide the integrand of Eq. (A.7) by P_u and by P_g . Thus we have for the speckle transfer function

$$\begin{aligned} \frac{\mathcal{T}(\vec{f})}{\mathcal{T}(0)} &= (\frac{1}{2} \pi)^{-2} \iint d\vec{x} d\vec{p} \mathcal{U}(\vec{x}) \mathcal{U}(\vec{x} + \vec{\alpha}) \mathcal{U}(\vec{x} - \vec{p}) \mathcal{U}(\vec{x} - \vec{p} + \vec{\alpha}) \\ &\times \exp[-6.88 (D/r_0)^{5/3} \Psi(\vec{p}, \vec{\alpha})] \frac{P_u(\vec{x})}{P_u(\vec{x})} \frac{P_g(\vec{p})}{P_g(\vec{p})} \quad . \end{aligned} \quad (A.15)$$

Making use of Eq. 's (A.13) and (A.14), this can be rewritten as

$$\begin{aligned} \frac{\tilde{J}(\vec{k})}{\tilde{J}(0)} = & \frac{32}{\pi} \sigma^3 h(1 - |\vec{\alpha}|) \iint d\vec{x} d\vec{p} P_u(\vec{x}) P_e(\vec{p}) \\ & \times \left\{ \mathcal{N}(\vec{x}) \mathcal{N}(\vec{x} + \vec{\alpha}) \mathcal{N}(\vec{x} - \vec{p}) \mathcal{N}(\vec{x} - \vec{p} + \vec{\alpha}) \right. \\ & \left. \times \exp \left[\frac{1}{2} |\vec{p}|^2 / \sigma^2 - 6.88 (D/r_0)^{3/5} \Psi(\vec{p}, \vec{\alpha}) \right] \right\} . \end{aligned} \quad (\text{A.16})$$

The quantity in the large curly brackets is the modified integrand whose mean value, in accordance with the probability densities $P_u(\vec{x})$ and $P_e(\vec{p})$, we wish to determine by Monte Carlo random sampling.

Taking note of Eq. (A.10), we reason that we can minimize the effective variability of the modified integrand when $|\vec{\alpha}|$ is much larger than r_0/D by choosing the sampling parameter σ to make the argument of the exponential in the modified integrand vanish when $|\vec{p}|$ equals σ . This leads to the condition

$$\begin{aligned} \sigma &= (r_0/D) (1/6.88)^{3/5} \\ &= 0.207 (r_0/D) , \quad \text{for } |\vec{\alpha}| \gg (r_0/D) . \end{aligned} \quad (\text{A.17'})$$

If we now take note of Eq. (A.9), we see that when $|\vec{\alpha}|$ is much less than r_0/D , then the argument of the exponential in the modified integrand will have relatively little variation with \vec{p} if σ is comparatively large. So as to avoid taking too many samples outside the range in which $\mathcal{N}(\vec{x} - \vec{p})$ and $\mathcal{N}(\vec{x} - \vec{p} + \vec{\alpha})$ are non-zero, we somewhat arbitrarily suggest that the sampling parameter σ have the value

$$\sigma = \frac{1}{2} , \quad \text{for } |\vec{\alpha}| \ll (r_0/D) . \quad (\text{A.17''})$$

To smoothly combine Eq. 's (A. 17') and (A. 17''), we chose to use as the gaussian distribution sampling parameter

$$\sigma = \left\{ \frac{\left(\frac{|\vec{\alpha}|}{r_0/D} \right)^2 [0.207 (r_0/D)]^2 + \left(\frac{r_0/D}{|\vec{\alpha}|} \right)^2 \left[\frac{1}{2} \right]^2}{\left(\frac{|\vec{\alpha}|}{r_0/D} \right)^2 + \left(\frac{r_0/D}{|\vec{\alpha}|} \right)^2} \right\}^{1/2} \quad (\text{A. 17})$$

Given σ , it is a straightforward matter to generate appropriately distributed random samples of the two components of \vec{p} , namely, p_1 and p_2 according to the equation

$$p_1 = \sigma g_1 \quad ; \quad p_2 = \sigma g_2 \quad , \quad (\text{A. 18})$$

where g_1 and g_2 are gaussian distributed random variables with zero mean value and unity standard deviation. Well-defined computer routines for generating the random variables g_1 and g_2 exist. The generation of the random samples x_1 and x_2 follows from the equations

$$x_1 = \frac{1}{2} - |\vec{\alpha}| - (1 - |\vec{\alpha}|) u_1 \quad , \quad (\text{A. 19a})$$

$$x_2 = h (u_2 - \frac{1}{2}) \quad , \quad (\text{A. 19b})$$

where u_1 and u_2 are random variables uniformly distributed on the interval between zero and unity (0, 1). [Clearly x_1 and x_2 are uniformly distributed, and by substituting the limiting values of u_1 and u_2 , we can confirm that x_1 and x_2 just span the ranges defined by Eq. 's (A. 11a) and (A. 11b).]

If we use the notation $\text{MCA } \langle \vec{x}; p_1(\vec{x}) | \vec{y}; p_2(\vec{y}) \rangle \langle f(\vec{x}, \vec{y}) \rangle$ to denote the average value of the function $f(\vec{x}, \vec{y})$ when evaluated as a Monte Carlo Average over the sampling distributions of \vec{x} and \vec{y} defined by $p_1(\vec{x})$ and

$p_2(\vec{y})$, then it is obvious from consideration of Eq. (A.16) that we can write the speckle transfer function as

$$\begin{aligned} \frac{\tilde{J}(\vec{f})}{\tilde{J}(0)} \approx & \frac{32}{\pi} \sigma^2 h(1-|\vec{\alpha}|) \text{MCA} \left\{ \vec{x}; P_u(\vec{x}) | \vec{p}; P_e(\vec{p}) \parallel \right. \\ & \{ \mathcal{N}(\vec{x}) \mathcal{N}(\vec{x}+\vec{\alpha}) \mathcal{N}(\vec{x}-\vec{p}) \mathcal{N}(\vec{x}-\vec{p}+\vec{\alpha}) \\ & \left. \times \exp \left[\frac{1}{2} |\vec{p}|^2 / \sigma^2 - 6.88 (D/r_0)^{5/3} \psi(\vec{p}, \vec{\alpha}) \right] \right\} \end{aligned} \quad (\text{A.20})$$

We can estimate the variance of the modified integrand as

$$\begin{aligned} \text{Var} \approx & \frac{32}{\pi} \sigma^2 h(1-|\vec{\alpha}|) \text{MCA} \left\{ \vec{x}; P_u(\vec{x}) | \vec{p}; P_e(\vec{p}) \parallel \right. \\ & \{ \mathcal{N}(\vec{x}) \mathcal{N}(\vec{x}+\vec{\alpha}) \mathcal{N}(\vec{x}-\vec{p}) \mathcal{N}(\vec{x}-\vec{p}+\vec{\alpha}) \\ & \left. \times \exp \left[\frac{1}{2} |\vec{p}|^2 / \sigma^2 - 6.88 (D/r_0)^{5/3} \psi(\vec{p}, \vec{\alpha}) \right] \right\}^2 \\ & - [\tilde{J}(\vec{f})/\tilde{J}(0)]^2 \end{aligned} \quad (\text{A.21})$$

Accordingly, the standard deviation of the Monte Carlo estimate of the normalized bispectrum, $\tilde{J}(\vec{f})/\tilde{J}(0)$, which we obtain from Eq. (A.20) is

$$\text{SD} = (\text{Var}/C)^{1/2}, \quad (\text{A.22})$$

where C is the number of sample values of (\vec{x}, \vec{p}) that we used in forming the Monte Carlo Average.

In Appendix B, we list a computer program which generates a table of values for the speckle transfer function, $\tilde{J}(\vec{f})/\tilde{J}(0)$, and for the associated standard deviation, subject to the conditions that no more than one million samples will be used, and that otherwise the Monte Carlo sampling process

will stop as soon as an estimated one-percent accuracy for the speckle transfer function is achieved. Results were calculated for values of D/r_0 equal to 10 , 30 , 100 , 300 , and 1000, and for a very large range of values of the normalized spatial frequency, $\vec{\alpha} = \lambda \vec{f}/D$, from very near zero to very near unity. The choice of values for the magnitude of $\vec{\alpha}$ was made to match a gaussian distribution scale so as to provide fine detail for $|\vec{\alpha}|$ near zero, as well as for $|\vec{\alpha}|$ near unity. The speckle transfer function values, $J(\vec{f})/J(0)$, are listed in Table A.1 . In Table A.2, we show the ratio of the standard deviation to the estimated value along with the number of samples used to form that estimated value for each entry in Table A.1. In evaluating the speckle transfer function, random samples were used in blocks of one-thousand, the number of blocks used being adjusted to provide one-percent accuracy, except that no more than one thousand blocks were ever used.

We recall that our objective in this appendix was to provide a basis for testing the accuracy of the approximations to the speckle transfer function provided by Eq. (40) for large values of $|\vec{\alpha}|$ relative to r_0/D , and by Eq. (44) for small values of $|\vec{\alpha}|$ relative to r_0/D . Accordingly, our computer program also calculated these approximation results. In Fig.'s 1 to 5, we have plotted the Monte Carlo estimates of the speckle transfer function as a function of the normalized spatial frequency, $|\vec{\alpha}| = \lambda |\vec{f}|/D$, for each of the five values of D/r_0 considered, along with the corresponding approximation results of Eq.'s (40) and (44). As can be seen from a consideration of these figures, the approximations are each quite good in their region of expected validity. This is particularly so for the larger values of D/r_0 .

Table A. 1

Speckle Transfer Function
Monte Carlo Results

Normalized Spatial Frequency $ \xi $	Speckle Transfer Function				
	$D/r_0 = 10$	$D/r_0 = 30$	$D/r_0 = 100$	$D/r_0 = 300$	$D/r_0 = 1000$
0.00021	9.96e-01	9.92e-01	9.83e-01	9.28e-01	6.14e-01
0.00026	1.00e-00	1.00e-00	9.67e-01	8.87e-01	5.01e-01
0.00032	1.01e-00	9.93e-01	9.81e-01	8.59e-01	3.72e-01
0.00040	9.99e-01	9.95e-01	9.65e-01	8.27e-01	2.44e-01
0.00050	9.88e-01	9.89e-01	9.58e-01	7.62e-01	1.34e-01
0.00062	9.89e-01	9.93e-01	9.34e-01	6.75e-01	5.71e-02
0.00077	9.80e-01	9.91e-01	9.07e-01	5.73e-01	1.74e-02
0.00096	9.96e-01	9.81e-01	8.83e-01	4.62e-01	3.15e-03
0.00119	9.96e-01	9.72e-01	8.25e-01	3.29e-01	2.00e-04
0.00147	9.96e-01	9.63e-01	7.57e-01	2.09e-01	1.16e-05
0.00182	9.78e-01	9.42e-01	6.88e-01	1.10e-01	1.21e-06
0.00225	9.64e-01	9.24e-01	5.95e-01	4.47e-02	7.54e-07
0.00278	9.53e-01	8.95e-01	4.90e-01	1.26e-02	8.95e-07
0.00343	9.59e-01	8.56e-01	3.63e-01	2.32e-02	7.84e-07
0.00422	9.52e-01	8.25e-01	2.50e-01	2.40e-04	7.83e-07
0.00516	9.54e-01	7.63e-01	1.48e-01	2.69e-05	6.80e-07
0.00634	9.33e-01	6.87e-01	7.12e-02	1.28e-05	6.93e-07
0.00774	9.02e-01	5.99e-01	2.71e-02	1.02e-05	6.49e-07
0.00943	8.74e-01	4.92e-01	7.61e-03	9.25e-06	6.05e-07
0.01144	8.36e-01	3.90e-01	1.58e-03	8.50e-06	6.06e-07
0.01364	7.81e-01	2.89e-01	3.30e-04	8.27e-06	5.73e-07
0.01608	7.16e-01	1.91e-01	1.32e-04	7.58e-06	5.67e-07
0.01882	6.62e-01	1.13e-01	1.04e-04	7.47e-06	5.55e-07
0.02294	5.65e-01	5.75e-02	8.89e-05	7.03e-06	5.42e-07
0.02849	5.11e-01	2.61e-02	8.22e-05	6.91e-06	5.20e-07
0.03377	4.26e-01	1.05e-02	7.63e-05	6.50e-06	5.22e-07
0.03933	3.33e-01	4.21e-03	7.17e-05	6.46e-06	5.33e-07
0.04677	2.50e-01	2.10e-03	6.84e-05	6.15e-06	4.95e-07
0.05464	1.90e-01	1.39e-03	6.72e-05	6.03e-06	4.90e-07
0.06353	1.30e-01	1.10e-03	6.25e-05	5.90e-06	4.72e-07
0.07350	8.42e-02	9.68e-04	5.93e-05	5.77e-06	4.55e-07
0.08461	5.36e-02	8.83e-04	5.79e-05	5.53e-06	4.53e-07
0.09691	3.50e-02	8.09e-04	5.51e-05	5.43e-06	4.36e-07
0.11046	2.24e-02	7.57e-04	5.35e-05	5.26e-06	4.23e-07
0.12529	1.60e-02	7.15e-04	5.07e-05	4.99e-06	4.19e-07
0.14142	1.20e-02	6.69e-04	4.86e-05	4.86e-06	3.89e-07
0.15888	9.92e-03	6.34e-04	4.67e-05	4.65e-06	3.83e-07
0.17766	8.33e-03	5.95e-04	4.43e-05	4.45e-06	3.74e-07
0.19777	7.38e-03	5.67e-04	4.20e-05	4.27e-06	3.65e-07
0.21919	6.53e-03	5.42e-04	4.08e-05	4.12e-06	3.48e-07
0.24189	5.83e-03	5.03e-04	3.78e-05	3.85e-06	3.33e-07
0.26583	5.24e-03	4.83e-04	3.66e-05	3.70e-06	3.19e-07
0.29094	5.09e-03	4.65e-04	3.46e-05	3.44e-06	3.02e-07
0.31716	4.63e-03	4.23e-04	3.20e-05	3.30e-06	2.87e-07
0.34570	3.91e-03	3.54e-04	2.83e-05	2.95e-06	2.51e-07
0.42233	3.57e-03	3.05e-04	2.50e-05	2.56e-06	2.26e-07
0.47826	2.71e-03	2.63e-04	2.13e-05	2.20e-06	1.94e-07
0.53364	2.25e-03	2.16e-04	1.80e-05	1.94e-06	1.63e-07
0.58893	1.79e-03	1.77e-04	1.50e-05	1.57e-06	1.39e-07
0.64260	1.45e-03	1.42e-04	1.23e-05	1.25e-06	1.13e-07
0.69345	1.09e-03	1.15e-04	9.81e-06	1.03e-06	9.94e-08
0.74067	8.37e-04	8.97e-05	7.55e-06	8.00e-07	6.92e-08
0.78374	6.16e-04	6.72e-05	5.64e-06	6.23e-07	5.31e-08
0.82234	4.36e-04	4.97e-05	4.31e-06	4.54e-07	4.04e-08
0.85633	3.01e-04	3.60e-05	3.10e-06	3.35e-07	2.92e-08
0.88571	2.02e-04	2.44e-05	2.21e-06	2.39e-07	2.08e-08
0.91062	1.23e-04	1.64e-05	1.53e-06	1.66e-07	1.44e-08
0.93129	7.40e-05	1.07e-05	1.30e-06	1.10e-07	9.77e-09
0.94809	4.01e-05	6.82e-06	9.51e-07	7.34e-08	6.53e-09
0.96145	2.01e-05	3.93e-06	4.11e-07	4.54e-08	4.02e-09
0.97183	9.46e-06	2.21e-06	2.47e-07	2.87e-08	2.63e-09
0.97974	4.18e-06	1.11e-06	1.45e-07	1.69e-08	1.55e-09
0.98563	1.75e-06	5.34e-07	9.37e-08	1.01e-08	9.26e-10
0.99994	6.88e-07	2.33e-07	4.35e-08	5.77e-09	5.27e-10

Table A.2

Monte Carlo Error Parameters

For each of the Monte Carlo results shown in Table A.1 we show here our estimate of the rms fractional error, σ , and the number thousands of samples, C , required to achieve this fractional error. Because we never allowed use of more than one-million samples ($C=1000$), our worst case fractional error was 19.5% ($SD=0.195$), but for the most part a 1% ($SD=0.01$) fractional error was achieved, generally with only about 37,000 ($C=37$) samples in the Monte Carlo estimation process.

Normalized Spatial Frequency $ f $	$D/r_0 = 10$		$D/r_0 = 30$		$D/r_0 = 100$		$D/r_0 = 300$		$D/r_0 = 1000$	
	SD	C	SD	C	SD	C	SD	C	SD	C
0.00021	0.010	37.	0.010	37.	0.010	37.	0.010	37.	0.010	37.
0.00026	0.010	37.	0.010	37.	0.010	37.	0.010	37.	0.010	37.
0.00032	0.010	37.	0.010	37.	0.010	37.	0.010	37.	0.010	37.
0.00040	0.010	37.	0.010	37.	0.010	37.	0.010	37.	0.010	37.
0.00050	0.010	37.	0.010	37.	0.010	37.	0.010	37.	0.010	37.
0.00062	0.010	37.	0.010	37.	0.010	37.	0.010	37.	0.010	37.
0.00077	0.010	37.	0.010	37.	0.010	37.	0.010	37.	0.010	37.
0.00096	0.010	37.	0.010	37.	0.010	37.	0.010	37.	0.010	37.
0.00119	0.010	37.	0.010	37.	0.010	37.	0.010	37.	0.010	37.
0.00147	0.010	37.	0.010	37.	0.010	37.	0.010	37.	0.010	37.
0.00182	0.010	37.	0.010	37.	0.010	37.	0.010	37.	0.010	37.
0.00225	0.010	37.	0.010	37.	0.010	37.	0.010	37.	0.010	37.
0.00274	0.010	37.	0.010	37.	0.010	37.	0.010	37.	0.010	37.
0.00343	0.010	37.	0.010	37.	0.010	37.	0.010	37.	0.010	37.
0.00422	0.010	37.	0.010	37.	0.010	37.	0.010	37.	0.010	37.
0.00518	0.010	37.	0.010	37.	0.010	37.	0.010	37.	0.010	37.
0.00634	0.010	37.	0.010	37.	0.010	37.	0.010	37.	0.010	37.
0.00774	0.010	37.	0.010	37.	0.010	37.	0.010	37.	0.010	37.
0.00943	0.010	37.	0.010	37.	0.010	37.	0.010	37.	0.010	37.
0.01144	0.010	37.	0.010	37.	0.010	37.	0.010	37.	0.010	37.
0.01384	0.010	37.	0.010	37.	0.010	37.	0.010	37.	0.010	37.
0.01668	0.010	37.	0.010	37.	0.010	37.	0.010	37.	0.010	37.
0.02002	0.010	37.	0.010	37.	0.010	37.	0.010	37.	0.010	37.
0.02394	0.010	37.	0.010	37.	0.010	37.	0.010	37.	0.010	37.
0.02849	0.010	37.	0.010	37.	0.010	37.	0.010	37.	0.010	37.
0.03377	0.010	37.	0.010	37.	0.010	37.	0.010	37.	0.010	37.
0.03983	0.010	37.	0.010	37.	0.010	37.	0.010	37.	0.010	37.
0.04677	0.010	37.	0.010	37.	0.010	37.	0.010	37.	0.010	37.
0.05464	0.010	37.	0.010	37.	0.010	37.	0.010	37.	0.010	37.
0.06353	0.010	37.	0.010	37.	0.010	37.	0.010	37.	0.010	37.
0.07350	0.010	37.	0.010	37.	0.010	37.	0.010	37.	0.010	37.
0.08461	0.010	37.	0.010	37.	0.010	37.	0.010	37.	0.010	37.
0.09691	0.010	37.	0.010	37.	0.010	37.	0.010	37.	0.010	37.
0.11046	0.010	37.	0.010	37.	0.010	37.	0.010	37.	0.010	37.
0.12529	0.010	37.	0.010	37.	0.010	37.	0.010	37.	0.010	37.
0.14142	0.010	37.	0.010	37.	0.010	37.	0.010	37.	0.010	37.
0.15886	0.010	37.	0.010	37.	0.010	37.	0.010	37.	0.010	37.
0.17766	0.010	37.	0.010	37.	0.010	37.	0.010	37.	0.010	37.
0.19777	0.010	37.	0.010	37.	0.010	37.	0.010	37.	0.010	37.
0.21919	0.010	37.	0.010	37.	0.010	37.	0.010	37.	0.010	37.
0.24139	0.010	37.	0.010	37.	0.010	37.	0.010	37.	0.010	37.
0.26583	0.010	37.	0.010	37.	0.010	37.	0.010	37.	0.010	37.
0.29094	0.010	37.	0.010	37.	0.010	37.	0.010	37.	0.010	37.
0.31716	0.010	37.	0.010	37.	0.010	37.	0.010	37.	0.010	37.
0.34470	0.010	37.	0.010	37.	0.010	37.	0.010	37.	0.010	37.
0.42283	0.010	37.	0.010	37.	0.010	37.	0.010	37.	0.010	37.
0.47826	0.010	37.	0.010	37.	0.010	37.	0.010	37.	0.010	37.
0.53304	0.010	37.	0.010	37.	0.010	37.	0.010	37.	0.010	37.
0.58893	0.010	37.	0.010	37.	0.010	37.	0.010	37.	0.010	37.
0.64260	0.010	37.	0.010	37.	0.010	37.	0.010	37.	0.010	37.
0.69345	0.010	37.	0.010	37.	0.010	37.	0.010	37.	0.010	37.
0.74067	0.010	37.	0.010	37.	0.010	37.	0.010	37.	0.010	37.
0.78374	0.010	37.	0.010	37.	0.010	37.	0.010	37.	0.010	37.
0.82234	0.010	37.	0.010	37.	0.010	37.	0.010	37.	0.010	37.
0.85633	0.010	37.	0.010	37.	0.010	37.	0.010	37.	0.010	37.
0.88571	0.010	37.	0.010	37.	0.010	37.	0.010	37.	0.010	37.
0.91062	0.010	37.	0.010	37.	0.010	37.	0.010	37.	0.010	37.
0.93129	0.010	37.	0.010	37.	0.010	37.	0.010	37.	0.010	37.
0.94809	0.010	37.	0.010	37.	0.010	37.	0.010	37.	0.010	37.
0.96145	0.010	37.	0.010	37.	0.010	37.	0.010	37.	0.010	37.
0.97153	0.010	37.	0.010	37.	0.010	37.	0.010	37.	0.010	37.
0.97974	0.010	37.	0.010	37.	0.010	37.	0.010	37.	0.010	37.
0.98553	0.010	37.	0.010	37.	0.010	37.	0.010	37.	0.010	37.
0.98994	0.010	37.	0.010	37.	0.010	37.	0.010	37.	0.010	37.

Computer Program Listings

Appendix B

Page 2

Monte Carlo Integral Evaluation

```

1  real m
2  dimension z(2),a(2),at(27,64)
3  tol(x)=(2./3.1415926)*(atan(sqrt((1./(x*x))-1.))-x*sqrt(1-x*x))
4  f(x)=1.-0.5*(((0.019527*x-0.200344)*x-0.115194)*x-0.196856)*x-1.)*(-41)
5  c16=1./6.
6  c13=1./3.
7  c56=5./6.
8  c53=5./3.
9  z1=1.03
10 z2=1.05
11 z3=0.01
12 n=0
13 at(1,1)=10.
14 at(1,2)=10.
15 at(1,3)=100.
16 at(1,4)=100.
17 at(1,5)=1000.
18 do 500 asd=-3.7,-0.475,0.075
19   n=n+1
20   if(asd.lt.0.) go to 600
21   at(2,n)=f(asd)
22   go to 601
23 600 asd=-asd
24   at(2,n)=1.-f(asd)
25   continue
26 500 continue
27 do 510 asd=-0.135,2.325,0.14
28   n=n+1
29   if(asd.lt.0.) go to 610
30   at(2,n)=f(asd)
31   go to 611
32 610 asd=-asd
33   at(2,n)=1.-f(asd)
34   continue
35 510 continue
36 do 700 ndr=1.5
37   drz=at(1,ndr)
38   do 800 n10r=1.64

```

```

39      alphasat(2,nalcha)
40      drs53=a.29*(drz+c53)
41      drsqrdrz
42      sigma=2.2074/drz
43      adrsaloha*drz
44      adrsatdrz*drz
45      at(5*drz-2,nalcha)=1.e-20
46      if(aloha.gt.5./drz) go to 900
47      expon=drz*3*aloha*c53
48      if(expon.lt.-50.) go to 900
49      at(5*drz-2,nalcha)=tdl(aloha)*tdl(aloha)*exp(expon)
50  900 continue
51      at(5*drz-1,nalcha)=1.e-20
52      if(aloha.gt.3.2/drz) at(5*drz-1,nalcha)=0.435*tdl(aloha)/drsqrdrz
53      sigma=2.*(adrsqrdrz+sigma-0.25/adrzsq)/(adrsqrdrz+1./adrsqrdrz)
54      if(drz.lt.2.1) sigma=0.5
55      asat1=aloha
56      n=drz*(1.-asat)
57      sigma=sqrt(0.5*sigma)
58      a53=aloha*c53
59      asat=0.5*asat
60      asat=0.1*asat
61      s=1.e-13
62      asat=0.
63      c=0.
64  110 call random_normal_seed(2)
65      o1=sigma*c(1)
66      o2=sigma*c(2)
67      o2sq=o2*o2
68      asat1=o1+o2sq
69  100 call random_uniform_seed(2)
70      c=c-1
71      s1=0.5-aloha*(aloha-1.)*c(1)
72      s2=s*(c(2)-0.5)
73      s2sq=s2*s2
74      asat1=s1+s2sq
75      if(asat1.gt.0.25) go to 310
76      s1=s1-aloha
77      if(s1sq=s1*o1+c2sq.gt.0.25) go to 310
78      s1=s1-c1
79      s2=s2-c2
80      smp2sq=s2*o2+c2sq
81      if(s1sq=s1*o1+c2sq.gt.0.25) go to 310
82      smp2sq=s1*o1-aloha
83      if(smp2sq=smp2sq+c2sq.gt.0.25) go to 310
84      if(asat1.gt.asat) go to 230
85      if(asat1.lt.asat) go to 210
86      asat1=aloha
87      asat1=aloha
88      o=(asat1-o2sq)*c53*(asat1+o2sq)*c53
89      o=(asat1/sigma)-(asat1*c53-a53-0.5*c53)*drz53
90
91      enze
92      if(en.lt.-40.) o=0.
93      if(en.lt.-40.) go to 300
94      o=exp(o)
95      go to 300
96  200 ctsq=pi*aloha
97      ctsq=ctsqrdrz/(asat+asat)
98      o=(asat/sigma)-drz53*(a53-c53*(asat/asat+c16)*(1.-c13*ctsqrdrz))
99      enze
100      if(en.lt.-40.) o=0.
101      if(en.lt.-40.) go to 300
102      o=exp(o)
103      go to 300
104  210 ctsq=pi*aloha
105      ctsq=ctsqrdrz/(asat+asat)
106      o=(asat/sigma)-drz53*(asat*c53-c53*(asat/asat+c16)*(1.-c13*ctsqrdrz))
107      enze
108      if(en.lt.-40.) o=0.
109      if(en.lt.-40.) go to 300
110      o=exp(o)
111  300 s=s-o
112      s=s+o
113  310 if(z1=ifix(c/z1).ne.c) go to 110
114      m=s/c
115      adrsqrdrz=(abs(((sso/(c-1.))-m)/c))
116      if((adrsqrdrz.gt.23).and.(c.lt.23)) go to 110
117      at(5*drz,nalcha)=(16./3.1-15926)*sigma*c(1.-aloha)*m
118      at(5*drz-1,nalcha)=(16./3.1-15926)*sigma*c(1.-aloha)*m
119      at(5*drz-2,nalcha)=c
120      print *,03, drz,aloha,(at(5*drz-1,nalcha),i=-2,1),c
121      format(17x,f5.1,3x,f7.4,6x,4(e12.4,3x),5x,'c.0')
122  800 continue
123  700 continue
124      rewind 30
125      write(30) at
126      rewind 31
127      write(31) at
128      end

```

Table Generation

Main Program

```
1      dimension at(27.56),t(10)
2      rewind 31
3      read(31) at
4      print 100
5      100 format(5x,////////)
6      do 200 i=1.56
7          print 300, at(2.1),at(5.1),at(10.1),at(15.1),at(20.1),at(25.1)
8      300 format(20x,f10.5,6x,t05(e10.2,3x))
9      200 continue
10     write (6,400)
11     400 format("1"////////)
12     do 500 i=1.56
13     do 700 j=1.5
14         t(2*j-1)=at(5*j-1.1)/at(5*j.1)
15     700 t(2*j)=at(5*j-2.1)/1.e3
16         print 500, at(2.1),t(j),j=1.10)
17     500 format(20x,f10.5,5x,f5.3,x,f5.0,2x))
18     500 continue
19     end
```